Table 3. A list of 23 genes with SS-hypo-DMRs exhibiting 'high' expression in human iPS/ES cells.

TargetID	Gene name	Fold change of expression	DNA methylation level in iPS/ES cells	DNA methylation level in Diff. cells
cg07337598	*ANXA9, annexin A9*	5.53	0.294±0.023	0.712±0.014
cg24183173	*BCOR, BCL-6 interacting corepressor*	5.06	0.014±0.005	0.784±0.051
cg21207436	*C14orf115, hypothetical protein LOC55237*	63.49	0.052±0.005	0.442±0.036
cg22892904	*CBX2, chromobox homolog 2*	11.48	0.068±0.006	0.607±0.051
cg24754277	*DAPK1, death-associated protein kinase 1*	28.34	0.115±0.005	0.708±0.049
cg21629895	*DNMT3A, DNA cytosine methyltransferase 3 alpha*	12.88	0.452±0.011	0.769±0.039
cg02932167	*ECEL1, endothelin converting enzyme-like 1*	17.57	0.115±0.007	0.672±0.059
cg25431974	*ECEL1, endothelin converting enzyme-like 1*	17.57	0.125±0.013	0.674±0.093
cg04515567	*FOXH1, forkhead box H1*	55.88	0.602±0.014	0.855±0.006
cg04464446	*GAL, galanin preproprotein*	194.63	0.241±0.022	0.735±0.056
cg00943909	*GNAS, guanine nucleotide binding protein*	47.33	0.076±0.016	0.528±0.081
cg27661264	*GNAS, guanine nucleotide binding protein*	47.33	0.037±0.005	0.355±0.054
cg18741908	*GPR160, G protein-coupled receptor 160*	60.48	0.068±0.006	0.466±0.038
cg20674521	*KCNJ4, potassium inwardly-rectifying channel J4*	6.11	0.306±0.024	0.772±0.043
cg21129531	*LRRC4, netrin-G1 ligand*	7.04	0.027±0.004	0.788±0.058
cg06144905	*PIPOX, L-pipecolic acid oxidase*	42.97	0.100±0.015	0.558±0.080
cg13083810	*POU5F1, POU domain; class 5;*	559.14	0.563±0.025	0.919±0.009
cg27377213	*PPP1R16B, protein phosphatase 1 regulatory inhibitor subunit 16B*	65.86	0.097±0.009	0.796±0.102
cg19580810	*RAB25, member RAS oncogene family*	6.16	0.062±0.010	0.703±0.030
cg09243900	*RAB25, member RAS oncogene family*	6.16	0.105±0.013	0.595±0.031
cg06303238	*SALL4, sal-like 4*	227.35	0.013±0.005	0.736±0.075
cg06614002	*SOX10, SRY-box 10*	5.23	0.028±0.005	0.829±0.046
cg01029592	*SOX15, SRY-box 15*	10.19	0.174±0.011	0.692±0.032
cg10242476	*TDGF1, teratocarcinoma-derived growth factor 1*	2472.59	0.146±0.013	0.387±0.052
cg20277416	*TM7SF2, transmembrane 7 superfamily member 2*	5.23	0.380±0.017	0.833±0.027
cg05656364	*VAMP8, vesicle-associated membrane protein 8*	9.69	0.070±0.010	0.698±0.081

Fold change of expression: Fold change of expression of the listed gene in human iPS/ES cells against the expression level in differentiated cells.
doi:10.1371/journal.pone.0013017.t003

Table 3 have trimethylation solely on K4 (Fig. 3C). Six genes have no histone trimethylation on K4 and K27 and the rest have bivalent K4/K27 trimethylation (Fig. 3C).

Discussion

Our genome-wide DNA methylation analysis shows that iPS and ES cells have similar methylation status although DNA methylation status of AM-iPS cells was closer to that of MRC-iPS cells than to that of ES cells in a small fraction. Doi et al. reported 71 differential methylated regions covering 64 genes between human iPS cells and ES cells [23]. Comparison of 535 aberrant DMSs (overlapping, 155; MRC-iPS specific, 125; AM-iPS specific, 255) with Doi's data, six genes that are *HOXA9*, *A2BP1*, *FZD10*, *SOX2*, *PTPRT* and *HYPK* overlapped. The inconsistency of most DMSs may be due to the stochastic nature of aberrant methylation through the genome. Human iPS and ES cells have general hyper-methylated status compared with differentiated cells. Our present genome-wide study indicates that pluripotent stem cells are generally hyper-methylated at promoter regions in comparison with differentiated cells. In the SS-DMRs, the number of CpG sites on non-CpG islands is grater than those on CpG islands, suggesting that promoter regions on non-CpG islands were more affected during reprogramming towards pluripotent stem cells. This result is consistent with the suggestion by Fouse et al. (2008) [24] that DNA methylation in mouse ES cells primarily occurred on non-CpG island regions of promoters.

Gene ontology analysis shows that signal transduction and transmembrane are major keywords for SS-hyper-DMRs. Most genes with SS-hyper-DMRs relate to differentiation. Recent studies demonstrate that blocking the p53 and TGFß pathways improves efficiency of generation of iPS cells [25,26,27,28,29,30]. Some genes related to these pathways are included in SS-hyper-DMR. Approximately 70% of SS-hyper-DMR have no modification of H3K4 and H3K27, suggesting that most genes with SS-hyper-DMRs are rigorously turned off by DNA methylation. By combining these findings with the result of *DNMT3A*, *DNMT3B* and *DNMT3L* induction in iPS/ES cells, we suggest that SS-hyper-DMRs apparently include genes that play a role in differentiated cells. Moreover, they must be silenced by DNMTs to establish pluripotency. We then identified 43 genes with SS-hyper-DMRs from "genes significantly suppressed in iPS/ES cells" (Table S3B and S4). In particular, *GBP3* and *SP100* could be used as epigenetic markers for pluripotency.

In addition, we successfully determined 23 genes with SS-hypo-DMRs from "genes significantly expressed in iPS/ES cells" (Table 3 and Table S3A). Those genes may start to be induced by demethylation and a significant subset of genes that act for de-

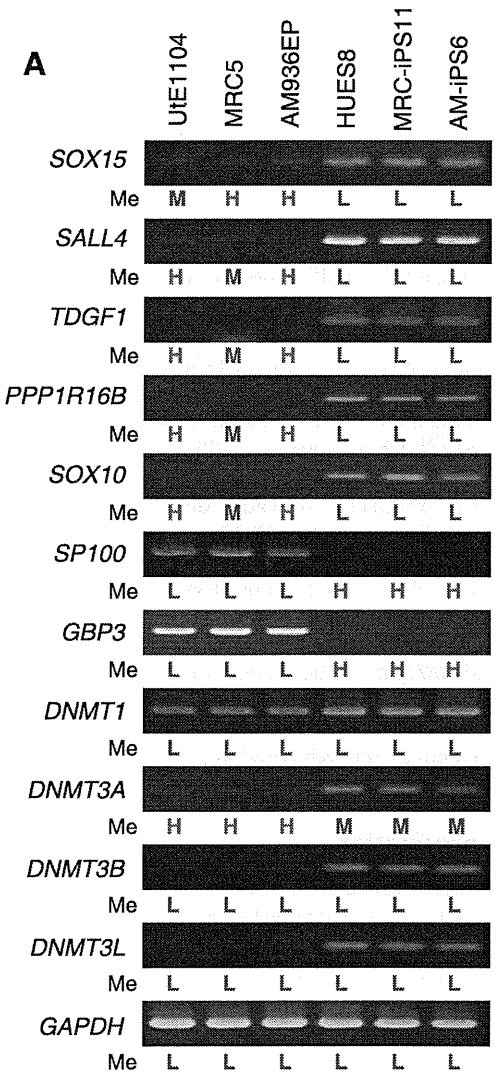

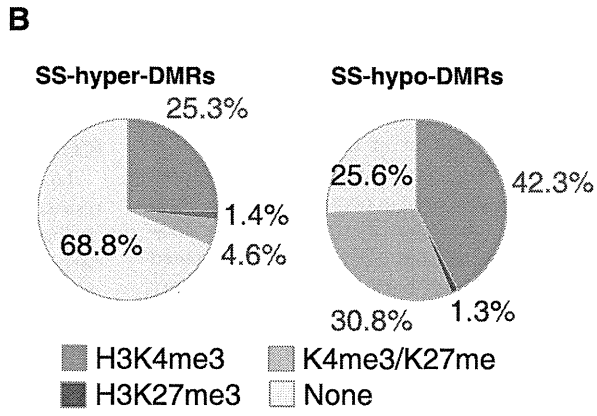

C

Histone modification of 23 genes in Table 3

H3K4me3		H3K4/K27me3	None
BCOR	C14orf115	ECL1	ANXA9
DAPK1	DNMT3A	GAL	PIPOX
GNAS	GPR160	KLNJ4	SALL4
PPP1R16B	RAB25	LRRC4	SOX10
SOX15	TDGF1		TM7SM2
POU5F1	FOXH1		VAMp8
CBX2			

Figure 3. Expression and histone modification of the SS-DMRs related genes. (**A**) Expression patterns of representative genes. RT-PCR analysis of 7 representative genes and methyltransferase genes. Methylation levels (Me) of each promoter are shown under each panel. H = High methylation (0.7<score); M = Middle methylation (0.3<score≤0.7); L = Low methylation (score≤0.3). (**B**) Comparable distribution of the SS-DMR and histone trimethylation (me3) of H3K4 and H3K27. Percentage of H3K4me3, H3K27me3, bivalent H3K4me3/K27me3 or non-modification on genes in SS-hyper-DMRs and in SS-hypo-DMRs. (**C**) Histone modification of 23 genes in Table 3.
doi:10.1371/journal.pone.0013017.g003

differentiation escape methylation in pluripotent stem cells during global reprogramming. Promoters of most marker genes expressed in human iPS/ES cells were low methylated in all cells examined (Table S5C). Analysis of histone modification of H3K4me3 and K27me3 from the database suggested that expression of *DNMT3B* might be regulated by methylation of H3K4 but expression of *DNMT3L* might not be under control of histone modification of H3K4me3 and K27me3. Most genes with SS-hypo-DMRs without expression in human iPS/ES cells have modification of H3K4me, bivalent H3K4me/K27me, or none, but do not have H3K27me3 modification. These genes may therefore be ready to be activated upon differentiation.

These findings are in generally consistent with the previous reports that have compared methylation profiles in somatic cells, iPS cells, and ES cells [23,31,32]. However, their analyses were limited only to human fibroblasts as a source for generation of iPS cells. In this study, we analyzed human extra-embryonic amnion cells and iPS cells. The DNA methylation profile at promoter sites clearly distinguished human pluripotent stem cells from differentiated cells. The SS-DMRs defined in this experiment can be used as a signature for "stemness". In addition, knowledge of the DNA methylation profile in human ES and iPS cells derived from different cell types is absolutely imperative and may allow us to screen for optimum iPS/ES cells and to validate and monitor iPS/ES cell derivatives for human therapeutic applications.

Materials and Methods

Human Cells

Human endometrium, bone marrow stroma, auricular cartilage, extra finger bone marrow, amnion, placental artery endothelium and menstrual blood cells were collected by scraping tissues from surgical specimens as a therapy, under signed informed consent, with ethical approval of the Institutional Review Board of the National Institute for Child Health and Development, Japan. Signed informed consent was obtained from

donors, and the surgical specimens were irreversibly de-identified. All experiments handling human cells and tissues were performed in line with Tenets of the Declaration of Helsinki. Endometrium (UtE1104), bone marrow stroma (H4-1) [33], auricular cartilage (Mim1508E), extra finger bone marrow (Yub636BM), amnion (AM936EP), placental artery endothelium (PAE551) and menstrual blood cell (Edom22) [34] cell lines were independently established in our laboratory. H4-1, Mim1508E, Yub636BM, AM936EP, Edom22, and MRC-5 [35] cells were maintained in the POWEREDBY10 medium (MED SHIROTORI CO., Ltd, Tokyo, Japan). PAE551 were cultured in EGM-2MV BulletKit (Lonza, Walkersville, MD, USA) containing 5% FBS. Human induced pluripotent stem (iPS) cells were generated, via procedures described by Yamanaka and colleagues [2] with slight modification. Human iPS cell lines derived from MRC-5 were designated as MRC-iPS cells [13], also iPS cell lines from AM936EP were named as AM-iPS cells [12]. Human iPS cells were maintained in iPSellon medium (Cardio Incorporated, Osaka, Japan) supplemented with 10 ng/ml recombinant human basic fibroblast growth factor (bFGF, Wako Pure Chemical Industries, Ltd., Osaka, Japan). Frozen pellets of human ES cell (HUESCs) were kindly gifted from Drs. C. Cowan and T. Tenzan (Harvard Stem Cell Institute, Harvard University, Cambridge, MA).

Illumina Infinium HumanMethylation27 BeadChip assay

Genomic DNA was extracted from cells using the QIAamp DNA Mini Kit (Qiagen). One microgram of genomic DNA from each sample was bisulfite-converted using EZ DNA Methylation-Gold kit (Zymo Research), according to the manufacturer's recommendations. Bisulfite-converted DNA was hybridized to the HumanMethylation27 BeadChip (Illumina inc.). Methylation levels of each CpG site were determined with fluorescent signals for methylated and unmethylated alleles. Methylated and unmethylated signals were used to compute a Beta value, which was a quantitative score of DNA methylation levels ranging from "0", for completely unmethylated, to "1", for completely methylated. On the HumanMethylation27 BeadChip, oligonucleotides for 27,578 CpG sites covering more than 14,000 genes are mounted, mostly selected from promoter regions. 26,956 (97.7%) out of the 27,578 CpG sites are set at promoters and 20,006 (72.5%) sites are set on CpG islands. CpG sites with $\geq$0.05 "Detection p value" (computed from the background based on negative controls) were eliminated from the data for further analysis, leaving 24,949 valid for use with the 16 samples tested.

Analysis of DNA methylation data

To analyze DNA methylation data, we used the following web tools: TIGR MeV [36] (http://www.tm4.org/mev.html) for hierarchical clustering heat map, NIA Array [37] (http://lgsun.grc.nia.nih.gov/ANOVA/) for hierarchical clustering that classify DNA methylation data by similarity and for principal component analysis (PCA) that finds major component in data variability, DAVID Bioinformatics Resources [38] (http://david.abcc.ncifcrf.gov/home.jsp), PANTHER Classification System [39] (http://www.pantherdb.org/), WebGestalt [40] (WEB-based GEne SeT AnaLysis Toolkit) (http://bioinfo.vanderbilt.edu/webgestalt/) based on based on KEGG (Kyoto Encyclopedia of Genes and Genomes) database [41] (http://www.genome.jp/kegg/) for gene ontology analysis, the GEO database (http://www.ncbi.nlm.nih.gov/geo/) for surveying gene expression in human iPS/ES cells (accession no. GSE9832 [16] and GSE12583 [17]), and the UCSC Genome Browser website [42] (http://genome.ucsc.edu/).

RT-PCR

RNA was extracted from cells using the RNeasy Plus Mini kit (Qiagen). An aliquot of total RNA was reverse transcribed using random hexamer primers. The cDNA template was amplified using specific primers for *SOX10*, *SOX15*, *PPP1R16B*, *SALL4*, *TDGF1*, *Sp100* and *GBP3*. Expression of glyceraldehyde-3-phosphate dehydrogenase (GAPDH) was used as a positive control. Primers used in this study are summarized in Table S6A.

Quantitative combined bisulfite restriction analysis (COBRA) and bisulfite sequencing

To confirm DNA methylation state, bisulfite PCR-mediated restriction mapping (known as the COBRA method) was performed. Sodium bisulfite treatment of genomic DNA was carried out as described above. PCR amplification was performed using IMMOLASE^{TM} DNA polymerase (Bioline Ltd; London, UK) and specific primers (Table S6B). After digestion with restriction enzymes, HpyCH4IV or Taq I, quantitative-COBRA coupled with the Shimadzu MCE®-202 MultiNA platform (Shimadzu, Japan) known as the Bio-COBRA method was carried out for quantitative DNA methylation level. Information of primers and restriction enzyme is summarized in Table S6B. To determine the methylation status of individual CpG in *SOX15*, *SALL4*, *Sp100* and *GBP3*, the PCR product was gel extracted and subcloned into pGEM T Easy vector (Promega, Madison, WI), and then sequenced. Methylation sites were visualized and quality control was carried out by the web-based tool, "QUMA" (http://quma.cdb.riken.jp/) [43].

Supporting Information

Table S1 Frequency of methylation states in each cell line.
Found at: doi:10.1371/journal.pone.0013017.s001 (0.04 MB PDF)

Table S2 A list of genes with SS-hyper-DMRs and SS-hypo-DMRs on KEGG Pathway.
Found at: doi:10.1371/journal.pone.0013017.s002 (0.05 MB PDF)

Table S3 (A) DNA methylation states of 23 genes (26 CpG sites) in Table 3, (B) DNA methylation states of 43 genes (50 CpG sites) in Table S4.
Found at: doi:10.1371/journal.pone.0013017.s003 (1.61 MB PDF)

Table S4 A list of 43 genes with SS-hyper-DMRs exhibiting 'low' expression in human iPS/ES cells.
Found at: doi:10.1371/journal.pone.0013017.s004 (0.07 MB PDF)

Table S5 (A) DNA methylation states of DNA methyltransferases, (B) Histone methylation states of DNA methyltransferases, (C) DNA methylation states of marker genes in human iPS/ES cells.
Found at: doi:10.1371/journal.pone.0013017.s005 (0.57 MB PDF)

Table S6 (A) primers used for RT-PCR, and (B) primers used for COBRA.
Found at: doi:10.1371/journal.pone.0013017.s006 (0.52 MB PDF)

Data set S1 A list of overlapped aberrant DMSs.
Found at: doi:10.1371/journal.pone.0013017.s007 (0.16 MB XLS)

Data set S2 A list of MRC-iPS specific aberrant DMSs.

Found at: doi:10.1371/journal.pone.0013017.s008 (0.13 MB XLS)

Data set S3 A list of AM-iPS specific aberrant DMSs.
Found at: doi:10.1371/journal.pone.0013017.s009 (0.25 MB XLS)

Data set S4 A list of SS-hyper-DMRs.
Found at: doi:10.1371/journal.pone.0013017.s010 (0.61 MB XLS)

Data set S5 A list of SS-hypo-DMRs.
Found at: doi:10.1371/journal.pone.0013017.s011 (0.10 MB XLS)

References

1. Thomson JA, Itskovitz-Eldor J, Shapiro SS, Waknitz MA, Swiergiel JJ, et al. (1998) Embryonic stem cell lines derived from human blastocysts. Science 282: 1145–1147.
2. Takahashi K, Tanabe K, Ohnuki M, Narita M, Ichisaka T, et al. (2007) Induction of pluripotent stem cells from adult human fibroblasts by defined factors. Cell 131: 861–872.
3. Huangfu D, Osafune K, Maehr R, Guo W, Eijkelenboom A, et al. (2008) Induction of pluripotent stem cells from primary human fibroblasts with only Oct4 and Sox2. Nat Biotechnol 26: 1269–1275.
4. Dimos JT, Rodolfa KT, Niakan KK, Weisenthal LM, Mitsumoto H, et al. (2008) Induced pluripotent stem cells generated from patients with ALS can be differentiated into motor neurons. Science 321: 1218–1221.
5. Woltjen K, Michael IP, Mohseni P, Desai R, Mileikovsky M, et al. (2009) piggyBac transposition reprograms fibroblasts to induced pluripotent stem cells. Nature 458: 766–770.
6. Li E (2002) Chromatin modification and epigenetic reprogramming in mammalian development. Nat Rev Genet 3: 662–673.
7. Reik W (2007) Stability and flexibility of epigenetic gene regulation in mammalian development. Nature 447: 425–432.
8. Hattori N, Nishino K, Ko YG, Ohgane J, Tanaka S, et al. (2004) Epigenetic control of mouse Oct-4 gene expression in embryonic stem cells and trophoblast stem cells. J Biol Chem 279: 17063–17069.
9. Nishino K, Hattori N, Tanaka S, Shiota K (2004) DNA methylation-mediated control of Sry gene expression in mouse gonadal development. J Biol Chem 279: 22306–22313.
10. Zingg JM, Pedraza-Alva G, Jost JP (1994) MyoD1 promoter autoregulation is mediated by two proximal E-boxes. Nucleic Acids Res 22: 2234–2241.
11. Tada M, Takahama Y, Abe K, Nakatsuji N, Tada T (2001) Nuclear reprogramming of somatic cells by in vitro hybridization with ES cells. Curr Biol 11: 1553–1558.
12. Nagata S, Toyoda M, Yamaguchi S, Hirano K, Makino H, et al. (2009) Efficient reprogramming of human and mouse primary extra-embryonic cells to pluripotent stem cells. Genes Cells 14: 1395–1404.
13. Makino H, Toyoda M, Matsumoto K, Saito H, Nishino K, et al. (2009) Mesenchymal to embryonic incomplete transition of human cells by chimeric OCT4/3 (POU5F1) with physiological co-activator EWS. Exp Cell Res 315: 2727–2740.
14. Cowan CA, Klimanskaya I, McMahon J, Atienza J, Witmyer J, et al. (2004) Derivation of embryonic stem-cell lines from human blastocysts. N Engl J Med 350: 1353–1356.
15. Brena RM, Auer H, Kornacker K, Plass C (2006) Quantification of DNA methylation in electrofluidics chips (Bio-COBRA). Nat Protoc 1: 52–58.
16. Park IH, Zhao R, West JA, Yabuuchi A, Huo H, et al. (2008) Reprogramming of human somatic cells to pluripotency with defined factors. Nature 451: 141–146.
17. Aasen T, Raya A, Barrero MJ, Garreta E, Consiglio A, et al. (2008) Efficient and rapid generation of induced pluripotent stem cells from human keratinocytes. Nat Biotechnol 26: 1276–1284.
18. Sperger JM, Chen X, Draper JS, Antosiewicz JE, Chon CH, et al. (2003) Gene expression patterns in human embryonic stem cells and human pluripotent germ cell tumors. Proc Natl Acad Sci U S A 100: 13350–13355.
19. Barski A, Cuddapah S, Cui K, Roh TY, Schones DE, et al. (2007) High-resolution profiling of histone methylations in the human genome. Cell 129: 823–837.
20. Mikkelsen TS, Ku M, Jaffe DB, Issac B, Lieberman E, et al. (2007) Genome-wide maps of chromatin state in pluripotent and lineage-committed cells. Nature 448: 553–560.
21. Bibikova M, Laurent LC, Ren B, Loring JF, Fan JB (2008) Unraveling epigenetic regulation in embryonic stem cells. Cell Stem Cell 2: 123–134.
22. Zhao XD, Han X, Chew JL, Liu J, Chiu KP, et al. (2007) Whole-genome mapping of histone H3 Lys4 and 27 trimethylations reveals distinct genomic compartments in human embryonic stem cells. Cell Stem Cell 1: 286–298.
23. Doi A, Park IH, Wen B, Murakami P, Aryee MJ, et al. (2009) Differential methylation of tissue- and cancer-specific CpG island shores distinguishes human induced pluripotent stem cells, embryonic stem cells and fibroblasts. Nat Genet 41: 1350–1353.
24. Fouse SD, Shen Y, Pellegrini M, Cole S, Meissner A, et al. (2008) Promoter CpG methylation contributes to ES cell gene regulation in parallel with Oct4/Nanog, PcG complex, and histone H3 K4/K27 trimethylation. Cell Stem Cell 2: 160–169.
25. Hong H, Takahashi K, Ichisaka T, Aoi T, Kanagawa O, et al. (2009) Suppression of induced pluripotent stem cell generation by the p53-p21 pathway. Nature 460: 1132–1135.
26. Kawamura T, Suzuki J, Wang YV, Menendez S, Morera LB, et al. (2009) Linking the p53 tumour suppressor pathway to somatic cell reprogramming. Nature 460: 1140–1144.
27. Utikal J, Polo JM, Stadtfeld M, Maherali N, Kulalert W, et al. (2009) Immortalization eliminates a roadblock during cellular reprogramming into iPS cells. Nature 460: 1145–1148.
28. Marion RM, Strati K, Li H, Murga M, Blanco R, et al. (2009) A p53-mediated DNA damage response limits reprogramming to ensure iPS cell genomic integrity. Nature 460: 1149–1153.
29. Li H, Collado M, Villasante A, Strati K, Ortega S, et al. (2009) The Ink4/Arf locus is a barrier for iPS cell reprogramming. Nature 460: 1136–1139.
30. Maherali N, Hochedlinger K (2009) Tgfbeta Signal Inhibition Cooperates in the Induction of iPSCs and Replaces Sox2 and cMyc. Curr Biol 18: 1718–1723.
31. Bibikova M, Chudin E, Wu B, Zhou L, Garcia EW, et al. (2006) Human embryonic stem cells have a unique epigenetic signature. Genome Res 16: 1075–1083.
32. Deng J, Shoemaker R, Xie B, Gore A, LeProust EM, et al. (2009) Targeted bisulfite sequencing reveals changes in DNA methylation associated with nuclear reprogramming. Nat Biotechnol 27: 353–360.
33. Mori T, Kiyono T, Imabayashi H, Takeda Y, Tsuchiya K, et al. (2005) Combination of hTERT and bmi-1, E6, or E7 induces prolongation of the life span of bone marrow stromal cells from an elderly donor without affecting their neurogenic potential. Mol Cell Biol 25: 5183–5195.
34. Cui CH, Uyama T, Miyado K, Terai M, Kyo S, et al. (2007) Menstrual blood-derived cells confer human dystrophin expression in the murine model of Duchenne muscular dystrophy via cell fusion and myogenic transdifferentiation. Mol Biol Cell 18: 1586–1594.
35. Jacobs JP, Jones CM, Baille JP (1970) Characteristics of a human diploid cell designated MRC-5. Nature 227: 168–170.
36. Saeed AI, Sharov V, White J, Li J, Liang W, et al. (2003) TM4: a free, open-source system for microarray data management and analysis. Biotechniques 34: 374–378.
37. Sharov AA, Dudekula DB, Ko MS (2005) A web-based tool for principal component and significance analysis of microarray data. Bioinformatics 21: 2548–2549.
38. Huang da W, Sherman BT, Lempicki RA (2009) Systematic and integrative analysis of large gene lists using DAVID bioinformatics resources. Nat Protoc 4: 44–57.
39. Mi H, Lazareva-Ulitsky B, Loo R, Kejariwal A, Vandergriff J, et al. (2005) The PANTHER database of protein families, subfamilies, functions and pathways. Nucleic Acids Res 33: D284–288.
40. Zhang B, Kirov S, Snoddy J (2005) WebGestalt: an integrated system for exploring gene sets in various biological contexts. Nucleic Acids Res 33: W741–748.
41. Kanehisa M, Araki M, Goto S, Hattori M, Hirakawa M, et al. (2008) KEGG for linking genomes to life and the environment. Nucleic Acids Res 36: D480–484.
42. Kent WJ, Sugnet CW, Furey TS, Roskin KM, Pringle TH, et al. (2002) The human genome browser at UCSC. Genome Res 12: 996–1006.
43. Kumaki Y, Oda M, Okano M (2008) QUMA: quantification tool for methylation analysis. Nucleic Acids Res 36: W170–175.

Acknowledgments

We would like to express our sincere thanks to Drs. M. Yamada and K Miyado for discussion and critical reading of the manuscript, to Drs. C. Cowan and T. Tenzan for HUES cell lines, to Dr. D. Kami for establishing the PAE551 cell line, to K. Miyamoto for bisulfite sequencing, to Drs. K. Hata and K. Nakabayashi for COBRA.

Author Contributions

Conceived and designed the experiments: KN AU. Performed the experiments: KN MT MYI. Analyzed the data: KN YT. Contributed reagents/materials/analysis tools: KN MT MYI HM YF EC YM HO NK HA. Wrote the paper: KN AU.

Biomed Microdevices (2010) 12:1097–1105
DOI 10.1007/s10544-010-9464-8

Enhanced effects of secreted soluble factor preserve better pluripotent state of embryonic stem cell culture in a membrane-based compartmentalized micro-bioreactor

Mohammad Mahfuz Chowdhury · Takeshi Katsuda · Kevin Montagne · Hiroshi Kimura · Nobuhiko Kojima · Hidenori Akutsu · Takahiro Ochiya · Teruo Fujii · Yasuyuki Sakai

Published online: 1 September 2010

Abstract Pluripotent stem cells are under the influence of soluble factors in a diffusion dominant *in vivo* microenvironment. In order to investigate the effects of secreted soluble factors on embryonic stem cell (ESC) behavior in a diffusion dominant microenvironment, we cultured mouse ESCs (mESCs) in a membrane-based two-chambered micro-bioreactor (MB). To avoid disturbing the cellular environment in the top chamber of the MB, only the culture medium of the bottom chamber was exchanged. Cell growth in the MB after 5 days of culture was similar to that in conventional 6-well plate (6-WP) and membrane-based Transwell insert (TW) cultures, indicating adequate nutrient supply in the MB. However, the cells retained higher expression of pluripotency markers (Oct4, Sox2 and Rex1) and secreted soluble factors (FGF4 and BMP4) in the MB. Inhibition of FGF4 activity in the MB and TW resulted in a similar cellular response. However, in contrast to the TW, inhibition of BMP4 activity revealed that autocrine action of the upregulated BMP4, which acted cooperatively with leukemia inhibitory factor (LIF), upregulated the pluripotency markers expression in the MB culture. We propose that BMP4 accumulated in the diffusion dominant microenvironment of the MB upregulated its own expression by a positive feedback mechanism—in contrast to the macro-scale culture systems—thereby enhancing the pluripotency of mESCs. The micro-scale culture platform developed in this study enables the investigation of the effects of soluble factors on ESCs in a diffusion dominant microenvironment, and is expected to be used to modulate the ESC fate choices.

Keywords Embryonic stem cell · Soluble factors · Diffusion · Microenvironment · Micro-bioreactor

M. M. Chowdhury (✉) · T. Katsuda · K. Montagne · H. Kimura · N. Kojima · T. Fujii · Y. Sakai
Institute of Industrial Science,
The University of Tokyo,
Tokyo, Japan
e-mail: mahfuz@iis.u-tokyo.ac.jp

K. Montagne · T. Fujii · Y. Sakai
LIMMS/CNRS-IIS, The University of Tokyo,
Tokyo, Japan

H. Akutsu
Department of Reproductive Biology,
National Research Institute for Child Health and Development,
Tokyo, Japan

T. Ochiya
Section for Studies on Metastasis,
National Cancer Center Research Institute,
Tokyo, Japan

1 Introduction

The autocrine and paracrine actions of soluble factors have an important role in directing pluripotent stem cell fate choices *in vivo* (Gadue et al. 2005; Loebel et al. 2003). Pluripotent stem cells and their progenies remain in a diffusion dominant microenvironment enclosed by the trophectoderm and extra-embryonic part until an appreciable amount of mass flow by convection occurs after the onset of blood circulation (Nagy et al. 2003). At the initial stage of embryo development, the fate of pluripotent cells is influenced by the adequate signaling

of soluble factors in the microenvironment. *In vitro*, ESC fate is also modulated by soluble factors (Kunath et al. 2007; Ying et al. 2003a). Although exogenous soluble factors can be added to the *in vitro* culture systems to control ESC fate, it is necessary to consider the influence of endogenous soluble factors which are secreted by the cells (Wiles and Proetzel 2006). This is highlighted by the fact that the addition of exogenous soluble factors has little influence on the initial differentiation of embryoid bodies (EBs) but influences the successive maturation of differentiated progenies towards the matured cell types (Ogawa et al. 2005; Wiles and Proetzel 2006). Furthermore, neuronal stem cells can be derived efficiently from mouse ESCs (mESCs) without the addition of exogenous factors (Ying et al. 2003b). Therefore, a culture system which mimics the diffusion dominant nature of the *in vivo* microenvironment is of great importance in order to improve our understanding of stem cell biology and control the stem cell fate decision (Loebel et al. 2003; Murry and Keller 2008).

Microfluidic technology provides advanced tools to develop micro-scale culture systems in an *in vivo* relevant dimension as well as to control mass transfer modes in the cellular microenvironment (Meyvantsson and Beebe 2008). Various micro-scale culture systems have been developed for ESC culture, but little is known about the effects of secreted soluble factors in these systems. Moreover, before proceeding to the differentiation of ESCs, it is necessary to characterize the differences between the micro and macro-scale cultures, namely regarding the effects of cell secreted soluble factors on ESC behavior. Human ESCs (hESCs) cells were cultured in straight micro-channels in static (Abhyankar et al. 2003) and semi-static (Korin et al. 2009) conditions. Although these cultures facilitated the accumulation of soluble factors around the cells owing to the diffusion dominant nature of static micro-scale culture, their effects on the cells were not investigated. Furthermore, the environment changed abruptly because of the daily replacement of the total culture medium. In micro-fabricated wells, hESCs were found to remain undifferentiated for more than two weeks (Mohr et al. 2006). The reason for that was not identified, but most likely resulted from soluble factors, cell-cell contacts and the extra-cellular matrix (ECM) produced by the cells. Some studies focused on controlling ESC microenvironment using perfusion-based systems (Figallo et al. 2007; Kim et al. 2006). In one of those studies, mESCs were cultured in microfluidic arrays at different flow rates, and the cell colonies showed flow-dependent size variations (Kim et al. 2006). This was attributed to the amount of nutrient delivery as well as the removal of waste and secreted factors. Although perfusion is a way to supply enough nutrients to cells for long-term culture and control the cellular microenvironment by removal of the secreted soluble factors, it disturbs the cellular diffusion-based microenvironment (Walker et al. 2004).

In this context, we developed a membrane-based two-chambered micro-bioreactor (designated as MB hereafter) and culture conditions for ESCs to investigate the influence of secreted soluble factors on cells by mimicking the diffusion-dominant *in vivo* microenvironment. The culture medium of the top chamber was not replaced during the culture period to avoid disturbance in the cellular microenvironment. In contrast, the culture medium of the bottom chamber was exchanged daily to maintain a sufficient nutrient supply. We cultured mESCs for five days in leukemia inhibitory factor (LIF) supplemented culture medium to study the effects of soluble factors on cellular behavior, such as cell-cell interactions, cell proliferation and differentiation, in which the influence of secreted soluble factors is important (Yu et al. 2005). In the LIF supplemented medium, BMP4 synergistically interacts with LIF to preserve the mESC pluripotency by resisting the differentiation inducing action of FGF4 (Ying et al. 2008c). Therefore, the cell states in the MB, membrane-based macro-scale Transwell Insert (TW) and conventional 6-well plate (6-WP) cultures were compared by the expression of pluripotency markers (Oct4, Sox2, Rex1 and Nanog) and cell secreted soluble factors (FGF4 and BMP4). In addition, we performed cell culture experiments by inhibiting signaling components of FGF4 and BMP4 in the MB and TW. Then, the gene expressions of inhibited and non-inhibited cultures were compared to discern the effects of soluble factors in the micro and macro-scale culture systems.

2 Materials and methods

2.1 Design of the MB

Figure 1 shows the design details of the MB. The reactor had two round chambers (top and bottom) with an area of 2.27 cm^2. They were kept separated by a porous membrane. Each of the chambers' height and volume were 500 μm and 114 μL, respectively. The chambers contained 13 pillars (1 mm in diameter) that kept the membrane horizontal, and enabled a more homogeneous cell seeding on the membrane. Cells were cultured on the top face of the membrane. To avoid culture area other than the membrane, two feeding holes in the top chamber were drilled at the chamber perimeter. On the other hand, feeding holes in the bottom chamber were made approximately 0.7 cm away from the chamber perimeter to get clearance from the membrane perimeter.

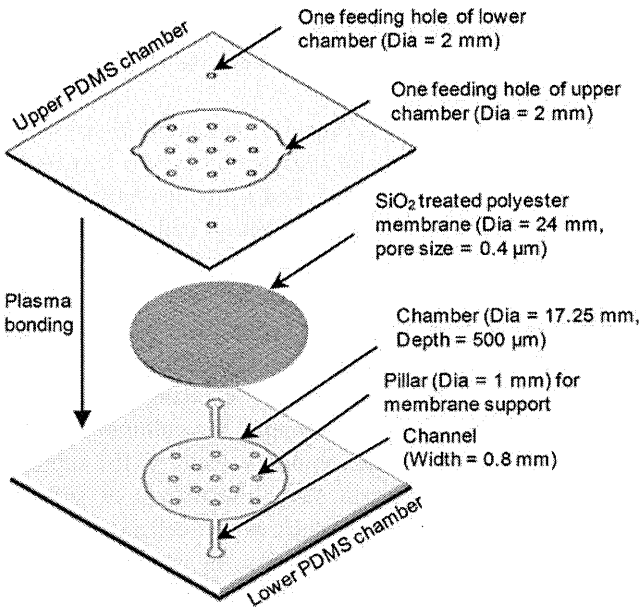

Fig. 1 Details of the PDMS chambers and membrane used to fabricate the MB. The membrane is sandwiched between the two PDMS chambers using the common O_2 plasma method. Both top and bottom PDMS chambers have two feeding holes to inject cells and exchange culture medium. Cells are cultured only on the top face of membrane

2.2 Fabrication of the MB

Details of the MB fabrication method are presented elsewhere (Kimura et al. 2008). Briefly, negative photoresist SU-8 2100 (Microchem Co.) was used to create the mold masters with the desired pattern. Then PDMS polymer (Silpot 184; Dow Corning Corp.) was mixed with its curing agent at a 10:1 ratio, poured over the mold masters, cured for 2 h at 75°C and peeled off thereafter.

The polyester membranes (pore size 0.4 μm, thickness 10 μm) were removed from Transwell Inserts 3450 (Corning Inc.). To bond the membrane with the PDMS layers, both sides of the membrane were coated with a thin layer of SiO_2 by sputtering for 20 s at 150 W and 0.5 Pa. The membrane was sandwiched between the two PDMS chambers following O_2 plasma treatment. Flow chips were then attached to the silicon tubing for connecting syringes; medium and reagents were manually introduced using those syringes.

2.3 Pre-treatment of experimental group (6-WP, TW and MB)

Because SiO_2 was used to coat the polyester membrane incorporated in the MB, the top side of the TW membrane was also coated with SiO_2 by sputtering. The TW and MB were then sterilized for 2 h under UV light. A 0.2% w/v gelatin solution was applied to cover the surface of the 6-WP and the membrane surfaces of the TW and MB, which was followed by 6 h of incubation. Culture medium for the experimental group was added to these culture systems for pre-incubation before seeding mESCs.

2.4 Routine cell culture

mESCs were routinely cultured in 60 mm gelatin coated dishes (Iwaki). Cell inoculation density was 2×10^4 cells/cm^2, and the cells were passaged every other day. Culture medium composition for routine culture was high glucose DMEM (DMEM; Gibco) containing 20% ESC qualified Fetal Bovine Serum (FBS; Gibco), 1000 U/ml ESGRO-LIF (Chemicon), 1% MEM non-essential amino acids (Gibco), 2 mM GlutaMax-I (Gibco), 100 U/ml penicillin, 100 U/ml streptomycin (Gibco) and 0.1 mM 2-mercaptoethanol (Gibco). The cells were maintained in a 37°C humidified environment containing 5% CO_2.

2.5 Cell culture in the experimental group

mESCs in the experimental group were cultured using the same medium as for routine culture except that DMEM and FBS were replaced with Knockout DMEM (Gibco) and 15% Knockout Serum (KSR; Gibco), respectively. KSR was used because it contains fewer extrinsic proteins. For the experimental group, cell inoculation density was 2×10^4 cells/cm^2. Cell culture in the experimental group was continued for 5 days. Culture medium of the 6-WP, the lower chambers of the TW and MB were changed daily. The upper chamber culture medium of the TW and MB were not changed. Morphological examination of the cells under microscope was performed daily. For inhibition experiments, Fibroblast Growth Factor Receptor (FGFR) antagonist SU5402 (Mohammadi 1997) (Calbiochem) at 10 μM and BMP4 antagonist Noggin (Smith and Harland 1992) (R&D Systems) at 100 ng/ml were added to the culture medium.

2.6 Glucose concentration measurement

Culture medium from the 6-WP, the lower chamber of the TW and MB were collected every day during the 5-day culture. On the 5th day, the culture medium from the upper chambers of the TW and MB were also collected. Glucose concentrations were measured with a glucose analyzer (GA05, A&T Corp., Japan).

2.7 Cell collection and qPCR analysis

Isolation of total mRNA was performed using Trizol Reagent (Invitrogen). In all culture systems, cells were dissociated using Trypsin (Gibco), counted and then lysed with Trizol. First-Strand cDNA Synthesis Kit (GE

Healthcare) was used to synthesize cDNA from the total mRNA. PCR reactions were carried out with a 7500 Real-Time PCR System (Applied Biosystems) using Quantitect SYBR Green PCR Kit (Qiagen). All steps were performed according to the manufacturers' instructions. Primers for cDNA amplification are listed in Table 1. qPCR were performed at least in duplicate. Raw data of PCR product amplification curves was analyzed using LinRegPCR v11.4 software (Ruijter et al. 2009) to determine the threshold cycles used in the $\Delta\Delta C_T$ method for relative quantification of gene expression. Geometric mean of the threshold cycles of reference genes GAPDH and β-Actin was used to normalize the target gene expressions. mESC culture at day 3 in the 6-WP was used as calibrator.

2.8 Statistical analysis

Student's *t*-test for comparing two groups and one way ANOVA with Tukey's post test for comparing more than two groups were performed for statistical evaluation using the demo version of GraphPad software (GraphPad Software, Inc.). Differences with a $P<0.05$ (*), $P<0.01$ (**), or $P<0.001$ (***) were considered to be statistically significant. All data are presented as the mean ± SEM.

3 Results

3.1 Effect of SiO_2 coating of the membranes on ESC behavior

SiO_2 coating on the membrane was necessary to bond it strongly with the PDMS layers, thereby preventing culture medium leakage in the MB. The coating did not affect permeability of the membranes as the measured glucose permeability of coated and non-coated membranes was the same (3×10^{-12} m^2s^{-1}). To examine whether the coating had any effect on cell behavior, we performed mESC culture on SiO_2-coated and non-coated membranes of the TW. Spread colonies of mESCs were observed on SiO_2-coated membranes (Fig. 2(a)), whereas these colonies remained spherical on the non-coated membranes (Fig. 2(b)). Cells attached weakly on the membranes without SiO_2 coating as the PBS wash during cell harvesting caused some cell loss. Consequently, the PBS wash was omitted for the non-coated membranes. However, no difference in cell growth was observed between SiO_2-coated and non-coated samples (fold changes in cell number relative to the seeded cells were 35.25±2.58 and 36.72±3.51, respectively). Furthermore, both of the cultures showed similar gene expression profile ($P>0.05$) (Fig. 3). Therefore, SiO_2 coating on the membrane was used for all the experiments.

3.2 Cell culture condition in the 6-WP, TW and MB

To keep the cellular microenvironment in the upper chamber of the MB and TW minimally disturbed, we only changed the culture medium of the lower chambers. Despite this, nutrients in these culture systems were sufficient as the glucose concentration throughout the 5 days of culture remained over half of the glucose concentration in fresh culture medium (0.02 M). Furthermore, no significant cell death was observed as assessed by the Trypan blue dye-exclusion test (data not shown) on day 5. Cell growth in all culture systems was similar ($P>0.05$) (Fig. 4). mESC culture in the TW and MB could be continued for more

Table 1 Genes and primers used in qPCR analyses

Genes	Description	Primer	Sequence (5′-3′)
GAPDH	Housekeeping gene	Forward	CAGAACATCATCCCTGCATC
		Reverse	CTGCTTCACCACCTTCTTGA
β-Actin	Housekeeping gene	Forward	TCACCCACACTGTGCCCATCTACGA
		Reverse	CAGCGGAACCGCTCATTGCCAATGG
Oct4	Pluripotency marker	Forward	AGAACCTTCAGGAGATATGC
		Reverse	TCTTCTCGTTGGGAATACTC
Sox2	Pluripotency marker	Forward	ACAAGGAAGGAGTTTATTCG
		Reverse	TTACCAACGATATCAACCTG
Rex1	Pluripotency marker	Forward	ACACAGAAGAAAGCAGGAT
		Reverse	GAACAATGCCTATGACTCAC
Nanog	Pluripotency marker	Forward	TGATTCTTCTACCAGTCCC
		Reverse	GGTCTTAACCTGCTTATAGC
FGF4	Cells' self-secreted soluble factor	Forward	TCGGTGTGCCTTTCTTTACC
		Reverse	ACCTTCATGGTAGGCGACAC
BMP4	Cells' self-secreted soluble factor	Forward	CCATCACGAAGAACATCTG
		Reverse	AATGTTTATACGGTGGAAGC

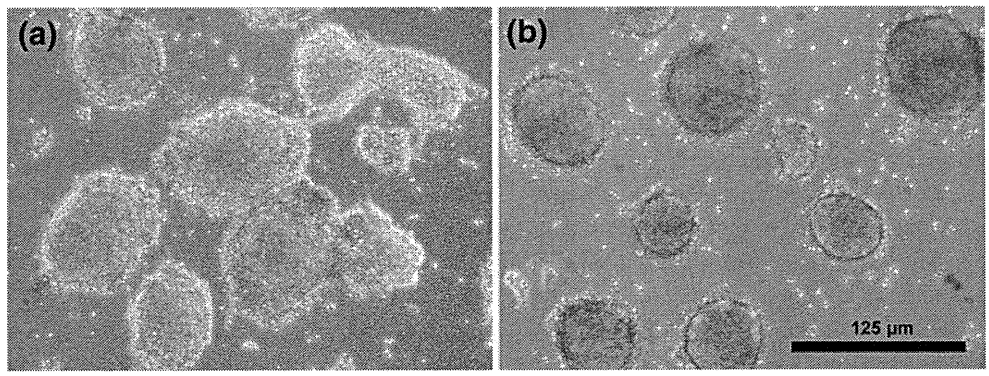

Fig. 2 mESC culture on day 5 on SiO_2-coated (**a**) or non-coated (**b**) polyester membranes of the TW. Cell colonies on the SiO_2-coated membrane are spread, whereas colonies on the non-coated membrane are round. Scale bar represents 125 μm

than 5 days, whereas cells began to die in the 6-WP after that period owing to nutrition depletion.

mESC colonies were extensively merged in the 6-WP (Fig. 5(a)) but they remained mostly as separated colonies in the TW and MB on day 5 (Fig. 5(b) and (c), respectively). Many differentiated cells showing a different morphology from usual mESCs were observed in the vicinity of cell colonies in the 6-WP and TW cultures (Fig. 5(d) and (e), respectively). In contrast, a few differentiated cells and smooth-bordered mESC colonies were observed in the MB (Fig. 5(f)), thereby indicating homogenous nature of the colonies.

3.3 Comparison of gene expression profiles among culture systems

In the MB culture, significantly higher expression levels of Oct4, Sox2 and Rex1 were observed compared to the 6-WP (Fig. 6). In addition, Sox2 and Rex1 expression in the MB were considerably higher than in the TW culture. These results showed that mESC pluripotency in the MB culture was higher than that in the macro-scale culture systems (6-WP and TW). Furthermore, both FGF4 and BMP4 were highly expressed in the MB culture compared to the TW (Fig. 6). However, only BMP4 expression in the MB was observed to be higher than in the 6-WP. Only Rex1 expression was different between the TW and 6-WP (Fig. 6).

3.4 Effects of soluble factors

To investigate whether dissimilarity in the activities of FGF4 and BMP4 between the MB and TW was responsible for the observed differences in the pluripotency markers expression (Sox2 and Rex1; Fig. 6), we performed inhibition experiments of FGF4 and BMP4 activities in the MB and TW cultures. FGF4 activity was inhibited using the small molecule SU5402, an antagonist of FGFR. This resulted in significantly increased expression of Nanog in the MB as well as TW cultures, but the other three pluripotency markers remained essentially unchanged (Fig. 7(a)). Expression of FGF4 increased, whereas that of BMP4 decreased in both MB and TW (Fig. 7(a)). We therefore concluded that the differentiation inducing activity of FGF4 suppressed Nanog expression, but did not affect the expression of Sox2 and Rex1 in the TW or MB. As a result, FGF4 cannot be

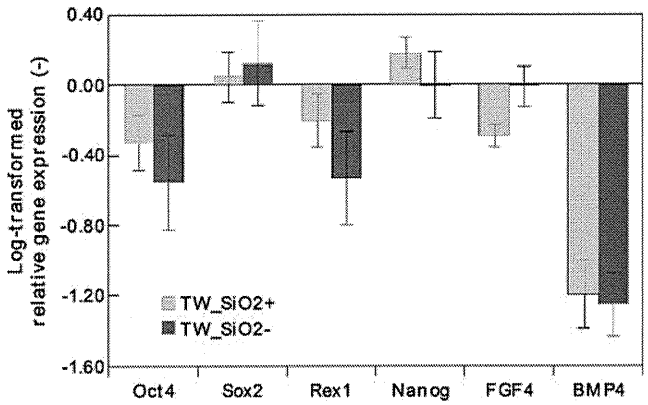

Fig. 3 Relative gene expression (Log_2-transformed) of mESCs cultured for 5 days on SiO_2-coated (TW_SiO2+) or non-coated (TW_SiO2−) membrane of the TW. Both cultures show similar gene expression profiles ($P>0.05$). Zero value represents the gene expression of mESC cultured in 6-WPs for 3 days. Columns and error bars represent mean ± SEM of three independent experiments

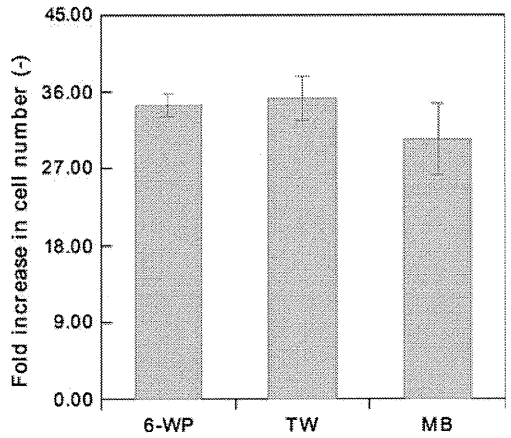

Fig. 4 Fold increase in cell number relative to the seeded cell number after 5 days of mESC culture in the 6-WP, TW and MB. Cell growths are similar in all culture systems ($P>0.05$). Columns and error bars represent mean ± SEM of four independent experiments

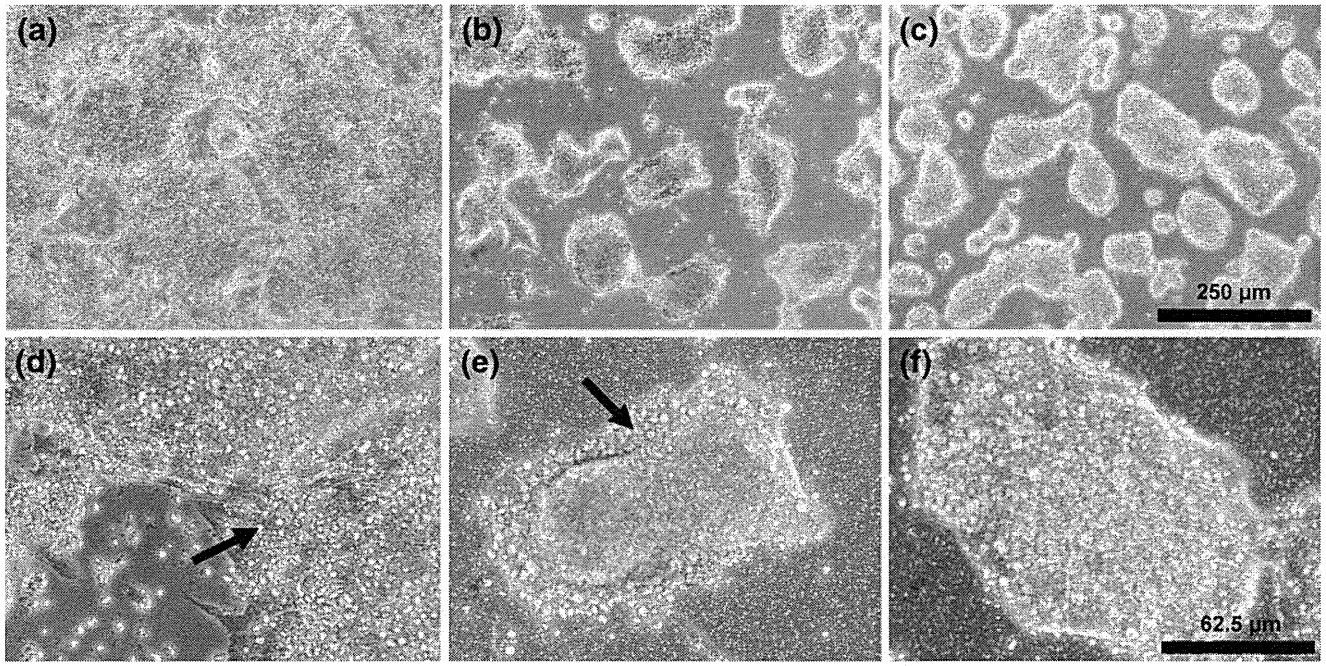

Fig. 5 mESC culture on day 5 in the 6-WP (**a**, **d**), TW (**b**, **e**) and MB (**c**, **f**). Arrows in the higher magnification images (**d**, **e**) indicate differentiated cells with a different morphology from the tightly packed colony type morphology of mESCs. Scale bars represents 250 μm (**a**, **b** and **c**), and 62.5 μm (**d**, **e** and **f**)

accounted for the differences in Sox2 and Rex1 expressions between the MB and TW cultures.

We then inhibited BMP4 activity using its antagonist Noggin. Expression of the pluripotency markers Sox2 and Rex1 decreased by the Noggin treatment in the MB, but they remained unchanged in the TW (Fig. 7(b)). In addition, both in the MB and TW culture, FGF4 and BMP4 expression remained unchanged by the same treatment. Sox2 and Rex1, which were upregulated more significantly in the MB as compared to the 6-WP and TW cultures (Fig. 6), decreased significantly by the Noggin treatment (Fig. 7(b)). Therefore, we can conclude that the activity of upregulated BMP4 (Fig. 6) is responsible for the better preservation of the mESC pluripotency in the MB.

4 Discussion

In this study, we developed a micro-scale culture system in which ESCs can be cultured in a diffusion dominant

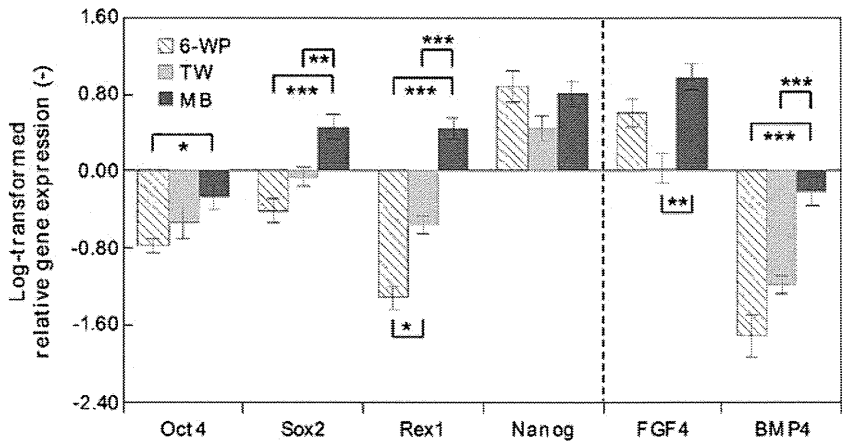

Fig. 6 Comparison of the gene expression profiles (Log_2-transformed) of mESCs cultured for 5 days in the 6-WP, TW and MB. Pluripotency markers (Oct4, Sox2 and Rex1) and soluble factors (FGF4 and BMP4) expression are upregulated in the MB. Zero represents gene expression of mESCs cultured in the 6-WP for 3 days. Columns and error bars represent mean ± SEM of six independent experiments. Statistical significance of the compared pairs are shown using the symbols *, ** and ***, representing *P*-values below 0.05, 0.01 and 0.001, respectively

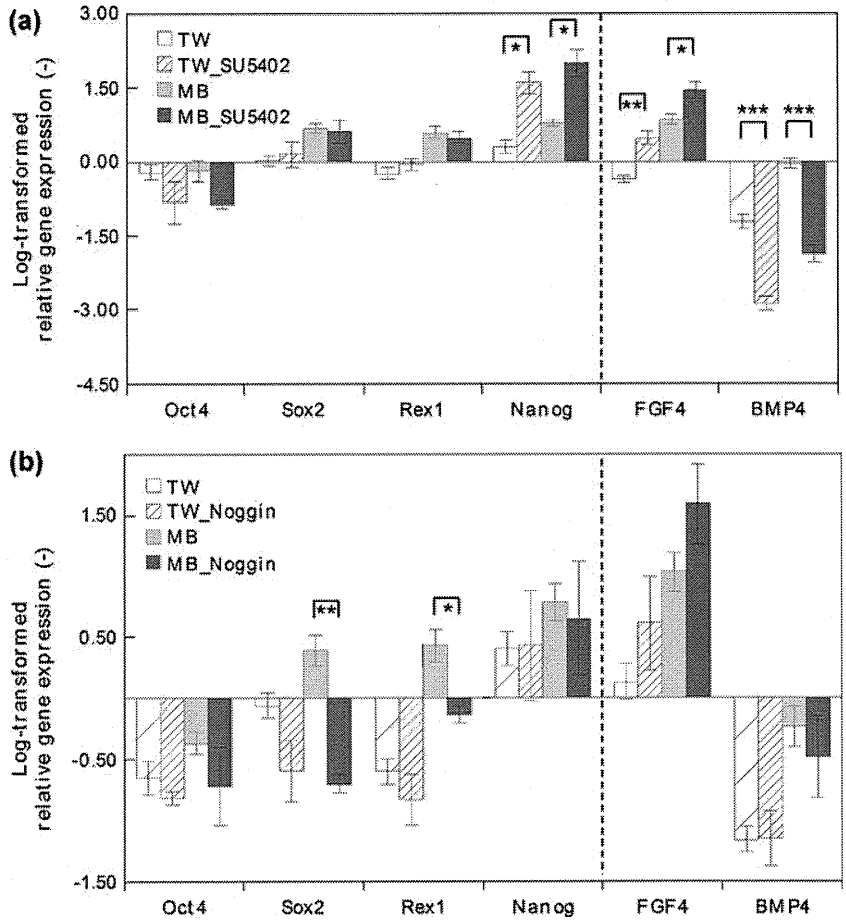

Fig. 7 Gene expression profiles (Log_2-transformed) of mESCs cultured for 5 days in the TW and MB, (**a**) with (TW_SU5402 and MB_SU5402) or without (TW and MB) inhibition of FGF4 signaling by SU5402; (**b**) with (TW_Noggin and MB_Noggin) or without (TW and MB) the BMP4 antagonist Noggin. Nanog expression both in the TW and MB increases following the SU5402 treatment. Sox2 and Rex1 expression decrease only in the MB following the Noggin treatment. Zero represents gene expression of mESCs cultured in 6-WP for 3 days. Columns and error bars represent mean ± SEM of four and three independent experiments for (a) and (b), respectively. Statistical significance of the compared pairs (TW against TW_SU5402; MB against MB_SU5402; TW against TW_Noggin; MB against MB_Noggin) are shown using symbols *, ** and ***, representing *P*-values below 0.05, 0.01 and 0.001, respectively

microenvironment without any limitation of nutrient supply for a long period of time. We observed better preservation of the mESC pluripotency in the micro-bioreactor than in the conventional macro-scale 6-WP and TW culture systems. We also demonstrated that autocrine effects of the up-regulated BMP4 cooperated with LIF to preserve the high pluripotency in the MB. Furthermore, the influence of FGF4 was similar in the TW and MB, whereas the influence of BMP4 was observed only in the MB.

A transcription network of Oct4, Sox2, Rex1 and Nanog maintains the pluripotency and proliferation of mESCs by suppressing the gene expression associated with differentiation (Masui et al. 2008; Niwa 2007). Usually, even in undifferentiated culture of mESCs in the presence of LIF, a proportion of the cells can undergo spontaneous differentiation (Smith 2001) which is associated with the decreased expression of those genes. Generally, overgrown differentiating mESC colonies have rough borders compared to the normal colonies. In the MB, mESC colonies were smooth-bordered, had few differentiated cells (Fig. 5(c) and (f)) and retained higher expression of the pluripotency markers (Fig. 6). These results indicated spontaneous differentiation of ESCs occurred less in the MB. Among the pluripotency markers, Sox2 and Rex1 showed prominently higher expression in the MB as compared to the WP and TW (Fig. 6). In fact, downregulation of Sox2 and Rex1 expression has a stronger correlation with loss of pluripotency of mESCs than the downregulation of Oct4 and Nanog expression (Palmqvist et al. 2005).

mESCs produce FGF4 extensively (Niwa et al. 2000) and BMP4 moderately (Johansson and Wiles 1995). FGF4 induces mESCs to differentiate (associated with the decreased expression of pluripotency markers of mESCs), which is counteracted by LIF and BMP4, as shown in Fig. 8 (Ying et al. 2008). In this study, although FGF4 was upregulated, high expression of BMP4 cooperated with LIF to preserve a high expression of pluripotency markers in the MB (Figs. 6, 7(b) and 8). In contrast, downregulated BMP4 in the TW had no observable effect on mESC pluripotecny markers, thereby maintaining a low level of pluripotency markers expression (Figs. 7(b) and 8). Notably, BMP4 expression was significantly upregulated only in the MB culture compared to the 6-WP and TW cultures (Fig. 6). Enclosed micro-scale environment might have facilitated the upregulation of BMP4 in the MB. Because the cell growth behaviors in these cultures were the same (Fig. 4), amount of secreted factors in the culture environment would be approximately the same. However, in the MB,

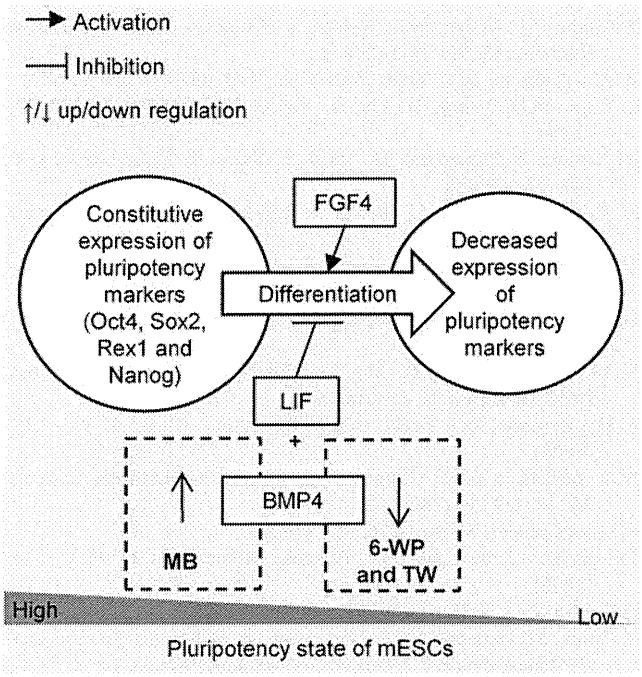

Fig. 8 A schematic diagram of the influence of soluble factors on the pluripotency markers in the embryonic stem cell culture environment. LIF and BMP4 cooperate to resist FGF4-induced differentiation. Effects of BMP4 on the pluripotency state of mESCs in the micro (MB) and macro-scale (TW) culture systems are also depicted

the culture volume was small (114 μL compared to the cell compartment volumes of 1.5 mL and 2 mL in the TW and 6-WP, respectively), and mass transfer was diffusion dominant due to small dimensions as well as the absence of a free interface between the culture medium and air (Yu et al. 2005). On the other hand, surface tension differences at the interface cause rapid convection in the macro-scale culture systems, and that creates a homogenous distribution of secreted soluble factors over the entire culture volume (Yu et al. 2005). Therefore, secreted soluble factors were accumulated and reached higher concentrations in the MB than in the 6-WP and TW. Moreover, they were presumably retained around the cell colonies at high concentrations for a longer time period in the MB owing to the diffusion dominant mass transfer. BMP4 can induce its own expression by a positive feedback mechanism (Vainio et al. 1993). Furthermore, owing to the relatively short half-life of BMP4, it is necessary to retain BMP4 near the cell for its activity (Miljkovic et al. 2008). Therefore, the higher exposure of cells to BMP4 in the MB culture than in the macro-scale cultures (the 6-WP and TW) may facilitate the feedback mechanism. This explains the observed upregulation and downregulation of BMP4 expression in the MB and macro-scale cultures, respectively (Fig. 6).

In spite of FGF4 accumulation, cells in the MB displayed a similar response in gene expression to that observed in the TW following FGF4 inhibition (Fig. 7(a)). However, inhibition of BMP4 activities resulted in significantly different effects in the MB and TW (Fig. 7(b)). Molecular diffusivities (inversely proportional to the cube root of molecular weight, MW) primarily determine the retention behavior of the soluble factors around the cells (Yu et al. 2005). FGF4 has a lower MW (22 kDa) than BMP4 (47 kDa), and may have diffused more quickly out of the cellular milieu. Therefore, it was unable to exert any influence on the cells as BMP4 did in the MB. In addition, extensively secreted FGF4 could have reached the threshold level of its activity equally in the MB and TW. These could be the plausible reason for the similar response observed in the TW and MB.

The average concentrations (total number of molecules divided by volume) of FGF4 and BMP4 in the MB might be the highest among the culture systems owing to the accumulation of these factors in the smallest volume. However, the cellular response to a soluble factor depends on the concentration level of the factor in the vicinity of the cell (local concentration). Both the average and local concentrations are influenced by various parameters of a soluble factor such as secretion, consumption, sequestration and release form the ECM. However, convection and diffusion only influence the local concentration. Owing to the diffusion dominant mass transfer in the MB, a soluble factor could be retained around the cells over time to reach a high concentration—all other parameters being the same in all culture systems. Therefore, in the MB, we could realize the combined effect of accumulation in a small volume and diffusion dominant mass transfer. However, we could not distinguish explicitly which concentration (average or local) reached the threshold level to impart a cellular response. To make the distinction, further investigation (experiments coupled with mathematical simulation) is necessary by taking the various parameters of a soluble factor into account along with diffusion and convection. This study, which characterizes the effects of soluble factors on ESC culture in the MB, provides a basis for the investigation.

mESCs secret FGF5, Nodal and BMP2 at low variable levels besides FGF4 and BMP4 (Wiles and Proetzel 2006). This micro-bioreactor and culture condition will be useful to study their effects in a diffusion dominant cellular environment, and will contribute to the understanding of ESC biology. The heterogeneity of ESCs during differentiation is one obstacle in obtaining lineage-specific cells useful for cell-based transplantation therapies (Singh and Terada 2007). Our micro-bioreactor can be used for obtaining relatively homogenous ESCs. In the absence of LIF, both FGF4 and BMP4 promote the differentiation of ESCs (Ying et al. 2003a). Therefore, the activity of soluble factors observed in the MB will provide an enhanced signaling microenvironment for controlling ESC differenti-

ation process in a monolayer format such as for neuronal (Ying et al. 2003b) or hepatocyte (Teratani et al. 2005) differentiation. By keeping the cellular environment in the upper chamber minimally disturbed, it is also possible to provide other soluble factors or inhibitors through the lower chamber to gain more precise control of the differentiation process.

5 Conclusions

In this study, we developed a membrane-based two-chambered micro-bioreactor for mESC culture to mimic the diffusion dominant mass transfer environment observed *in vivo*. The influence of soluble factors on cells in the micro-bioreator was compared with a macro-scale culture system. We observed enhanced retention of the pluripotent phenotype of mESCs in the micro-bioreactor owing to the enhanced effect of a soluble factor in a diffusion dominant microenvironment. A similar effect of the soluble factor was not observed in the macro-scale membrane-based Transwell insert culture system, in which soluble factors dissipated away from cell surrounding through inherent convection. This micro-bioreactor offers a suitable platform not only to understand the influence of secreted soluble factors on stem cell biology, but also to address an enhanced signaling environment to direct the ESC fate.

Acknowledgements M. M. Chowdhury was supported by Monbukagakusho scholarship from the Japan Ministry of Education, Culture, Sports, Science and Technology (MEXT). This research was supported in part by CREST from Japan Science and Technology Agency and GMSI (Global Center of Excellence for Mechanical Systems Innovation), The University of Tokyo. We would like to thank Dr. Masaki Nishikawa and Dr. Morgan Hamon for their useful suggestions regarding various technical aspects related to this study.

References

V.V. Abhyankar, G.N. Bittner, T.J. Kamp, D.J. Beebe, in 7th International Conference on Miniaturized Chemical and Biochemical Analysis Systems (Transducers Research Foundation, San Diego, California, USA, 2003), pp. 17–20.

E. Figallo, C. Cannizzaro, S. Gerecht, J.A. Burdick, R. Langer, N. Elvassore, G. Vunjak-Novakovic, Lab Chip **7**, 710–719 (2007)

P. Gadue, T.L. Huber, M.C. Nostro, S. Kattaman, G.M. Keller, Exp. Hematol. **33**, 955–964 (2005)

B.M. Johansson, M.V. Wiles, Mol. Cell. Biol. **15**, 141–151 (1995)

L. Kim, M.D. Vahey, H. Lee, J. Voldman, Lab Chip **6**, 394–406 (2006)

H. Kimura, T. Yamamoto, H. Sakai, Y. Sakai, T. Fujii, Lab Chip **8**, 741–746 (2008)

N. Korin, A. Bransky, U. Dinnar, S. Levenberg, Biomed. Microdev. **11**, 87–94 (2009)

T. Kunath, M.K. Saba-El-Leil, M. Almousailleakh, J. Wray, S. Meloche, A. Smith, Development **134**, 2895–2902 (2007)

D.A.F. Loebel, C.M. Watson, R.A.D. Young, P.P.L. Tam, Dev. Biol. **264**, 1–14 (2003)

S. Masui, S. Ohtsuka, R. Yagi, K. Takahashi, M.S. Ko, H. Niwa, BMC Dev. Biol. **8**, 45 (2008)

I. Meyvantsson, D.J. Beebe, Annu. Rev. Anal. Chem. **1**, 141–1427 (2008)

N.D. Miljkovic, G.M. Cooper, K.G. Marra, Osteoarthritis Cartilage **16**, 1121–1130 (2008)

M. Mohammadi, Science **276**, 955 (1997)

J.C. Mohr, J.J. de Pablo, S.P. Palecek, Biomaterials **27**, 6032–6042 (2006)

C.E. Murry, G. Keller, Cell **132**, 661–680 (2008)

A. Nagy, M. Gertsenstein, K. Vintersten, R. Behringer, *Manipulating the Mouse Embryo A Laboratory Manual*, 3rd edn. (Cold Spring Harbor, New York, 2003), pp. 32–38

H. Niwa, Development **134**, 635–646 (2007)

H. Niwa, J. Miyazaki, A.G. Smith, Nat. Genet. **24**, 372–376 (2000)

S. Ogawa, Y. Tagawa, A. Kamiyoshi, A. Suzuki, J. Nakayama, Y. Hashikura, S. Miyagawa, Stem Cells **23**, 903–913 (2005)

L. Palmqvist, C.H. Glover, L. Hsu, M. Lu, B. Bossen, J.M. Piret, R.K. Humphries, C.D. Helgason, Stem Cells **23**, 663–680 (2005)

J. M. Ruijter, C. Ramakers, W. M. H. Hoogaars, Y. Karlen, O. Bakker, M. J. B. van den Hoff, A. F. M. Moorman, Nucleic Acids Res. (2009) doi:10.1093/nar/gkp045

A.M. Singh, N. Terada, Trends Cardiovasc. Med. **17**, 96–101 (2007)

A.G. Smith, Annu. Rev. Cell Dev. Biol. **17**, 435–462 (2001)

W.C. Smith, R.M. Harland, Cell **70**, 829–840 (1992)

T. Teratani, H. Yamamoto, K. Aoyagi, H. Sasaki, A. Asari, G. Quinn, H. Sasaki, M. Terada, T. Ochiya, Hepatology **41**, 836–846 (2005)

S. Vainio, I. Karavanova, A. Jowett, I. Thesleff, Cell **75**, 45–58 (1993)

G.M. Walker, H.C. Zeringue, D.J. Beebe, Lab Chip **4**, 91–97 (2004)

M. V. Wiles, G. Proetzel, in *Embryonic Stem cells A Practical Approach*, ed. by E. Notarianni, M.J. Evans (Oxford University Press, New York, 2006), pp. 112–119

Q.L. Ying, J. Nichols, I. Chambers, A. Smith, Cell **115**, 281–292 (2003a)

Q.L. Ying, M. Stavridis, D. Griffiths, M. Li, A. Smith, Nat. Biotechnol. **21**, 183–186 (2003b)

Q.L. Ying, J. Wray, J. Nichols, L. Batlle-Morera, B. Doble, J. Woodgett, P. Cohen, A. Smith, Nature **453**, 519–524 (2008)

H. Yu, I. Meyvantsson, I.A. Shkel, D.J. Beebe, Lab Chip **5**, 1089–1095 (2005)

MTOpen

Efficient Generation of Hepatoblasts From Human ES Cells and iPS Cells by Transient Overexpression of Homeobox Gene *HEX*

Mitsuru Inamura[1,2], Kenji Kawabata[2,3], Kazuo Takayama[1,2], Katsuhisa Tashiro[2], Fuminori Sakurai[2], Kazufumi Katayama[1,2], Masashi Toyoda[4], Hidenori Akutsu[4], Yoshitaka Miyagawa[5], Hajime Okita[5], Nobutaka Kiyokawa[5], Akihiro Umezawa[4], Takao Hayakawa[6,7], Miho K Furue[8,9] and Hiroyuki Mizuguchi[1,2]

[1]Department of Biochemistry and Molecular Biology, Graduate School of Pharmaceutical Sciences, Osaka University, Osaka, Japan; [2]Laboratory of Stem Cell Regulation, National Institute of Biomedical Innovation, Osaka, Japan; [3]Department of Biomedical Innovation, Graduate School of Pharmaceutical Science, Osaka University, Osaka, Japan; [4]Department of Reproductive Biology, National Institute for Child Health and Development, Tokyo, Japan; [5]Department of Developmental Biology and Pathology, National Institute for Child Health and Development, Tokyo, Japan; [6]Pharmaceutics and Medical Devices Agency, Tokyo, Japan; [7]Pharmaceutical Research and Technology Institute, Kinki University, Osaka, Japan; [8]JCRB Cell Bank/Laboratory of Cell Culture, Department of Disease Bioresource, National Institute of Biomedical Innovation, Osaka, Japan; [9]Laboratory of Cell Processing, Institute for Frontier Medical Sciences, Kyoto University, Kyoto, Japan

Human embryonic stem cells (ESCs) and induced pluripotent stem cells (iPSCs) have the potential to differentiate into all cell lineages, including hepatocytes, *in vitro*. Induced hepatocytes have a wide range of potential application in biomedical research, drug discovery, and the treatment of liver disease. However, the existing protocols for hepatic differentiation of PSCs are not very efficient. In this study, we developed an efficient method to induce hepatoblasts, which are progenitors of hepatocytes, from human ESCs and iPSCs by overexpression of the *HEX* gene, which is a homeotic gene and also essential for hepatic differentiation, using a HEX-expressing adenovirus (Ad) vector under serum/feeder cell-free chemically defined conditions. Ad-HEX-transduced cells expressed α-fetoprotein (AFP) at day 9 and then expressed albumin (ALB) at day 12. Furthermore, the Ad-HEX-transduced cells derived from human iPSCs also produced several cytochrome P450 (CYP) isozymes, and these P450 isozymes were capable of converting the substrates to metabolites and responding to the chemical stimulation. Our differentiation protocol using Ad vector-mediated transient HEX transduction under chemically defined conditions efficiently generates hepatoblasts from human ESCs and iPSCs. Thus, our methods would be useful for not only drug screening but also therapeutic applications.

Received 18 March 2010; accepted 13 October 2010; published online 23 November 2010. doi:10.1038/mt.2010.241

INTRODUCTION

Human embryonic stem cells (ESCs) and induced pluripotent stem cells (iPSCs) are able to replicate indefinitely and differentiate into most cell types of the body,[1-4] and thereby have the potential to provide an unlimited source of cells for a variety of applications.[5] Hepatocytes are useful cells for biomedical research, regenerative medicine, and drug discovery. They are particularly applicable to drug screenings, such as for the determination of metabolic and toxicological properties of drug compounds in *in vitro* models, because the liver is the main detoxification organ in the body.[6] For these applications, it is necessary to prepare a large number of functional hepatocytes from human ESCs and iPSCs. Many of the existing methods for cell differentiation of human ESCs and iPSCs into hepatocytes employ undefined, serum-containing medium and feeder cells.[7-9] Preparation of human ESC- and iPSC-derived hepatocytes for therapeutic applications and drug toxicity testing in humans should be done in nonxenogenic culture systems to avoid potential contamination with pathogens. Furthermore, the efficiency of the differentiation of the human ESCs and iPSCs into hepatocytes is not particularly high using these methods.[9-14]

In vertebrate development, the liver is derived from the primitive gut tube, which is formed by a flat sheet of cells called the definitive endoderm.[5,15] Shortly afterwards, the definitive endoderm is separated into endoderm derivatives containing the liver bud, the cells of which are referred to as hepatoblasts. The hepatoblasts have the potential to proliferate and differentiate into both hepatocytes and cholangiocytes. In the process of hepatic differentiation, the maturation is characterized by the expression of liver- and stage-specific genes. For example, α-fetoprotein (AFP) is an early hepatic marker, which is expressed in hepatoblasts in the liver bud until birth, and its expression is dramatically reduced after birth.[16] In contrast, albumin (ALB), which is the most abundant protein synthesized by hepatocytes, is initially expressed at lower levels in early fetal hepatocytes, but its expression level is increased as the hepatocytes mature, reaching a maximum in adult hepatocytes.[17] Furthermore, isoforms of cytochrome P450 (CYP) proteins also exhibit differential expression levels according to the developmental stages

Correspondence: *Hiroyuki Mizuguchi, Department of Biochemistry and Molecular Biology, Graduate School of Pharmaceutical Sciences, Osaka University, 1-6 Yamadaoka, Suita, Osaka 565-0871, Japan. E-mail: mizuguch@phs.osaka-u.ac.jp*

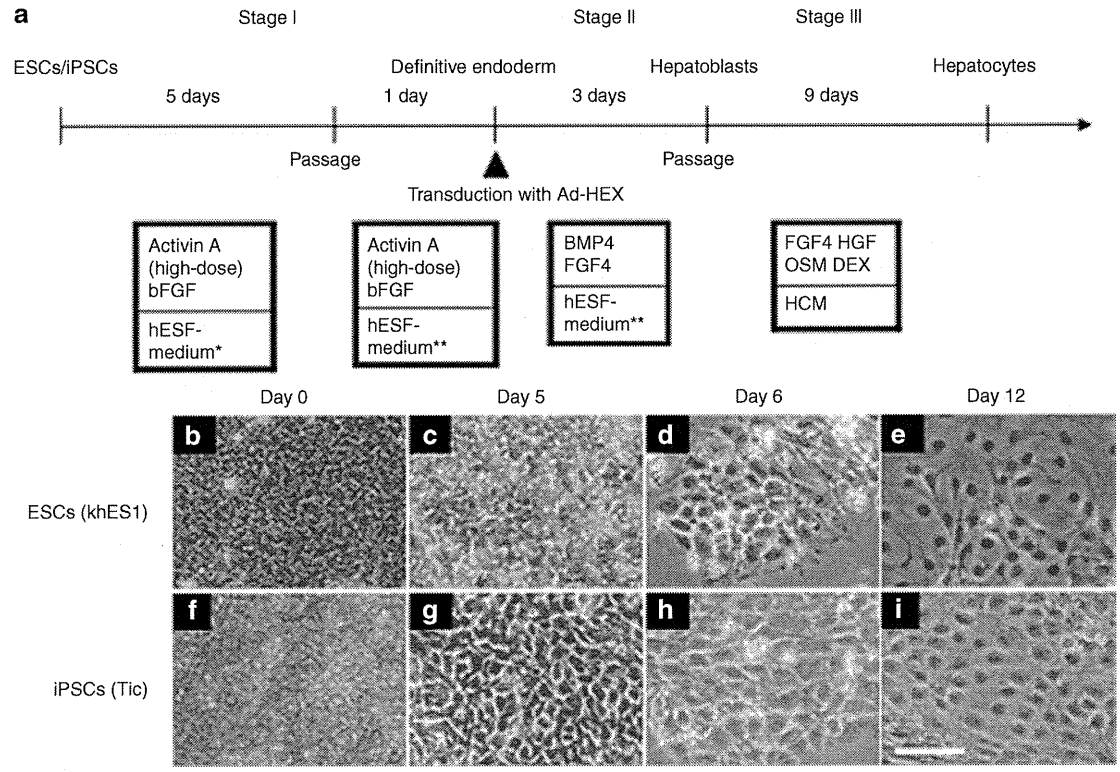

Figure 1 A strategy of differentiation of human embryonic stem cells (ESCs) and induced pluripotent stem cells (iPSCs) to hepatoblasts and hepatocytes. (**a**) Schematic representation illustrating the procedure for differentiation of human ESCs (khES1) and iPSCs (Tic) to hepatocytes. (**b–i**) Phase contrast microscopy showing sequential morphological changes (day 0–12) from (**b–e**) human ESCs (khES1) and (**f–i**) iPSCs (Tic) to hepatoblasts via the definitive endoderm. Bar = 50 μm. bFGF, basic fibroblast growth factor; BMP4, bone morphogenetic protein 4; DEX, dexamethasone; FGF4, fibroblast growth factor 4; HGF, hepatocyte growth factor; OSM, Oncostatin M; HCM, hepatocytes culture medium; *, hESF-GRO medium that was supplemented with 10 μg/ml human recombinant insulin, 5 μg/ml human apotransferrin, 10 μmol/l 2-mercaptoethanol, 10 μmol/l ethanolamine, 10 μmol/l sodium selenite, 0.5 mg/ml fatty acid free BSA; **, hESF-DIF medium that was supplemented with 10 μg/ml insulin, 5 μg/ml apotransferrin, 10 μmol/l 2-mercaptoethanol, 10 μmol/l ethanolamine, 10 μmol/l sodium selenite, 0.5 mg/ml BSA.

of the liver. Although most CYPs (including CYP3A4, CYP7A1, and CYP2D6) are only slightly expressed or not detected in the fetal liver tissue, the expression levels are dramatically increased after birth.[18]

For the development of hepatoblasts, numerous transcription factors are required, such as hematopoietically expressed homeobox (*HEX*), GATA-binding protein 6, prospero homeobox 1, and hepatocyte nuclear factor 4A.[15,19] Among them, *HEX* is suggested to function at the earliest stage of hepatic linage.[20] HEX is first expressed in the definitive endoderm and becomes restricted to the future hepatoblasts. Targeted deletion of the *HEX* gene in the mouse results in embryonic lethality and a dramatic loss of the fetal liver parenchyma.[19,21,22] The hepatic genes, including *ALB*, prospero homeobox1, and hepatocyte nuclear factor 4A, are transiently expressed in the definitive endoderm of *HEX*-null embryos, and further morphogenesis of the hepatoblasts does not occur.[23] In general, then, *HEX* is essential for the definitive endoderm to adopt a hepatic cell fate.

Adenovirus (Ad) vectors are one of the most efficient gene delivery vehicles and have been widely used in both experimental studies and clinical trials.[24] Ad vectors are attractive vehicles for gene transfer because they are easily constructed, can be prepared in high titers, and provide high transduction efficiency in both dividing and nondividing cells. We have developed efficient methods for Ad vector-mediated transient transduction into mouse ESCs and iPSCs.[25,26] We have also showed that the differentiations of mouse ESCs and iPSCs into adipocytes and osteoblasts were dramatically promoted by Ad vector-mediated peroxisome proliferator activated receptor γ and runt related transcription factor 2 transduction, respectively.[25,26]

In this study, we hypothesized that transient *HEX* transduction could efficiently induce hepatoblasts from human ESCs and iPSCs. A previous study demonstrated that *HEX* regulates the differentiation of hemangioblasts and endothelial cells from mouse ESCs,[27] whereas the role of *HEX* in the differentiation of hepatoblasts from human ESCs and iPSCs remains unknown. We found that differentiation of hepatoblasts from the human ESC- and iPSC-derived definitive endoderms, but not from undifferentiated human ESCs and iPSCs, could be facilitated by Ad vector-mediated transient transduction of a *HEX* gene. Furthermore, the Ad-HEX-transduced cells that were derived from human iPSCs were able to differentiate into functional hepatocytes *in vitro*. All the processes for cellular differentiation were performed under serum/feeder cell- free chemically defined conditions. Our culture systems and differentiation method based on Ad vector-mediated transient transduction under chemically defined conditions would provide a platform for drug screening as well as safe therapies.

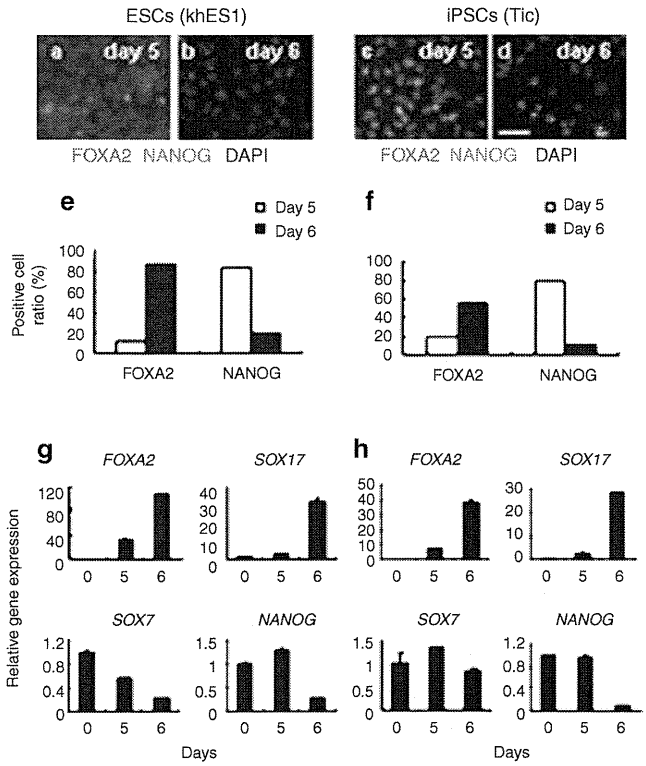

Figure 2 Characterization of the human ESC (khES1)- and iPSC (Tic) derived definitive endoderms. (**a–d**) The immunofluorescent staining of the human ESC (khES1)- and iPSC (Tic) derived differentiated cells before (**a** and **c**; day 5) and after passaging (**b** and **d**; day 6). The cells were immunostained with antibodies against FOXA2 and NANOG. Nuclei were stained with DAPI. (**e,f**) Semiquantitative analysis of the immunofluorescent staining in **a–d**. Data are presented as the mean of immunopositive cells counted in eight independent fields. (**g,h**) Real-time RT-PCR analysis of the level of definitive endoderm (*FOXA2* and *SOX17*), pluripotent (*NANOG*), and extra-embryonic endoderm (*SOX7*) gene expression at day 5 and 6. At day 5, the cells were passaged. Therefore, the data at day 5 and 6 show the levels of gene expression before (at day 5) or after the passage (at day 6). Data are presented as the mean ± SD from triplicate experiments. The graphs represent the relative gene expression level when the level of undifferentiated cells at day 0 was taken as 1. Bar = 50 μm. ESC, embryonic stem cells; iPSC, induced pluripotent stem cells.

RESULTS

Differentiation of human ESC- and iPSC-derived definitive endoderms

Our three-step differentiation protocol is illustrated in Figure 1a. After treatment with 50 ng/ml of Activin A (high-dose) and basic fibroblast growth factor (bFGF) for 5 days on a laminin-coated plate, morphologically, the human ESCs and iPSCs were gradually transformed from typical, defined, tight human ESC, and iPSC colonies (day 0) into less dense, flatter cells containing prominent nuclei (day 5), even though the majority of the cells had a morphology resembling that of undifferentiated cells (Figure 1b,c,f,g). FACS analysis showed that ~46% of human iPSC-derived differentiated cells expressed CXCR4 (expressed in the definitive endoderm but not the primitive endoderm) (**Supplementary Figure S1a**). Human ESC- and iPSC-derived differentiated cells were immunostained with the definitive endoderm marker, FOXA2 (Figure 2a,c). However, the majority of the cells expressed the pluripotent marker NANOG, indicating that undifferentiated cells remain in the induced cultures at day 5. After the cells were passaged with trypsin-EDTA and seeded on a laminin-coated plate a second time, the resultant cells were found to be more homogeneous and flatter at day 6 (Figure 1d,h). Semiquantitative analysis by counting immunopositive cells revealed that the number of FOXA2-positive cells was increased and, in turn, the number of NANOG-positive cells was decreased at day 6 after passaging (Figure 2e,f). Real-time reverse transcriptase (RT)-PCR analysis showed that the definitive endoderm markers *FOXA2* and *SOX17* mRNA were upregulated, whereas the pluripotent marker *NANOG* mRNA was downregulated at day 6 (Figure 2g,h). These results were consistent with the immunofluorescence results (Figure 2a–d). The expression levels of the mesoderm marker *FLK1* mRNA and ectoderm marker *PAX6* mRNA were downregulated or unchanged at day 6 (**Supplementary Figure S1b–e**). Importantly, the expression of *SOX7* mRNA (expressed in the extra-embryonic endoderm but not the definitive endoderm) was downregulated (Figure 2g,h). These results indicate that the definitive endoderm is induced or selected from human ESCs and iPSCs after passaging. We obtained the same results using another human iPSC line (**Supplementary Figure S2a–d**).

HEX induces hepatoblasts from the human ESC- and iPSC-derived definitive endoderms

To investigate whether forced expression of transcription factors could promote hepatic differentiation, the human ESC- and iPSC-derived definitive endoderms were transduced with Ad vectors. We used a fiber-modified Ad vector containing the elongation factor-1α promoter and a stretch of lysine residue (K7) peptides in the C-terminal region of the fiber knob to examine the transduction efficiency in the human ESC- and iPSC-derived definitive endoderms. The elongation factor-1α promoter was found to be highly active in human ESCs.[28] The K7 peptide targets heparan sulfates on the cellular surface, and the fiber-modified Ad vector containing K7 peptides was shown to be efficient for transduction into many kinds of cells.[29,30] The human ESC- and iPSC-derived definitive endoderms were transduced with a LacZ-expressing Ad vector (Ad-LacZ) at 3,000 vector particle/cell. X-Gal staining showed that the Ad-LacZ-transduced human ESC- and iPSC-derived definitive endoderms successfully expressed LacZ (Figure 3). Nearly 100% of the cells transduced with Ad-LacZ were strongly X-gal positive. The transduction efficiency in the human ESC- and iPSC-derived definitive endoderms transduced with the conventional Ad vector containing the wild-type capsid at 3,000 vector particle/cell was ~80% and X-gal staining was much weaker than that in the cells transduced with fiber-modified Ad vectors (**Supplementary Figure S6**).

Next, the human ESC- and iPSC-derived definitive endoderms were transduced with a HEX-expressing fiber-modified Ad vector (Ad-HEX). Although HEX is known to be a transcription factor that is essential for liver development, it remains unclear what the effect of transient *HEX* overexpression is on differentiation from human ESCs and iPSCs or their derivatives *in vitro*. We confirmed the overexpression of *HEX* in the human ESC- and iPSC-derived definitive endoderms transduced with Ad-HEX (**Supplementary Figure S3a–f**). Gene expression analysis revealed the upregulation of *AFP* mRNA, which was expressed by hepatoblasts or early hepatocytes, in Ad-HEX-transduced cells as

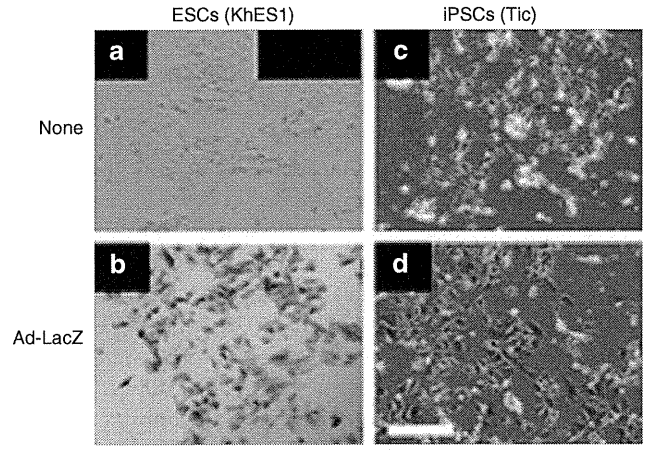

Figure 3 Efficient transgene expression in the human ESC (khES1)- and iPSC (Tic) derived definitive endoderms by using a fiber-modified Ad vector containing the EF-1α promoter. (**a,b**) Human ESC (khES1)-derived and (**c,d**) iPSC (Tic) derived definitive endoderms were transduced with 3,000 VP/cell of Ad-LacZ for 1.5 hours. The next day after transduction, X-gal staining was performed as described in the Materials and Methods section. Similar results were obtained in two independent experiments. Scale = 50 μm. Ad, adenovirus; EF-1α, elongation factor-1α; ESC, embryonic stem cells; iPSC, induced pluripotent stem cells; LacZ, Ad-LacZ-transduced cells; None, nontransduced cells.

compared with nontransduced cells or Ad-LacZ-transduced cells (**Figure 4a,c**). Expression of *ALB* mRNA, which is the most abundant protein in liver, was also observed in Ad-HEX-transduced cells (**Figure 4b,d**).

During liver development, both hepatocytes and cholangiocytes were differentiated from the hepatoblasts. We examined the protein expression of AFP, ALB, and the cholangiocyte marker cytokeratin 7 (CK7) in Ad-HEX-transduced cells by immunostaining (**Figure 4e–p**). The AFP-positive populations were detected in Ad-HEX-transduced cells (**Figure 4g,m**). ALB-positive cells were also detected, although the detection efficiency was very low (**Figure 4j,p**). CK7-positive cells were observed among the Ad-HEX-transduced cells, and all CK7-positive cells were found near the AFP- and ALB-positive cells, suggesting that hepatoblasts are generated by the transient overexpression of a *HEX* gene. Semiquantitative RT-PCR analysis showed that the expression levels of the liver-enriched transcription factors hepatocyte nuclear factor 1A, hepatocyte nuclear factor 1B, hepatocyte nuclear factor 4A, and hepatocyte nuclear factor 6 mRNA were upregulated in Ad-HEX-transduced cells (**Supplementary Figure S4a,b**). The expressions of CCAAT/enhancer binding protein α and prospero homeobox 1 mRNA, two transcription factors known to play a pivotal role in the establishment of the hepatoblasts, were also induced in Ad-HEX-transduced cells (**Supplementary Figure S4a, b**). Taken together, these findings indicate that *HEX* enhances the specification of hepatoblasts from the human ESC- and iPSC-derived definitive endoderms. Similar results were obtained with another human iPSC line (**Supplementary Figure S2e–g**).

Time course of differentiation of the definitive endoderm to hepatoblasts

Next, we examined the time course of AFP and CK7 expression during differentiation of human iPSCs to hepatoblasts in Ad-HEX-

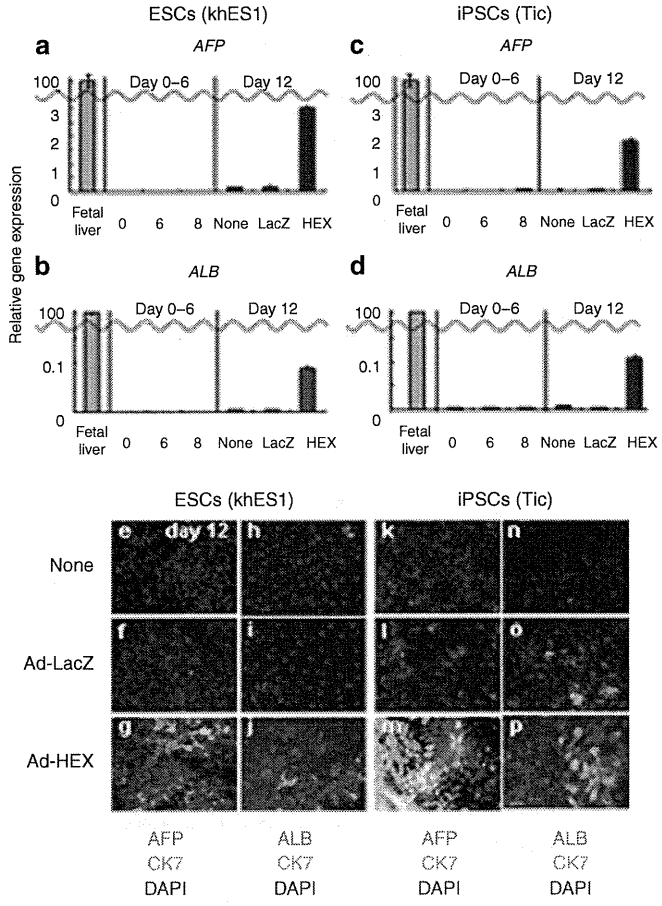

Figure 4 Efficient hepatoblast differentiation from the human ESC (khES1)- and iPSC (Tic) derived definitive endoderms by transduction of the *HEX* gene. (**a–d**) Real-time RT-PCR analysis of the level of (**a,c**) *AFP* and (**b,d**) *ALB* expression in nontransduced cells, Ad-LacZ-transduced cells, and Ad-HEX-transduced cells, all of which were induced from the human ESC (khES1)- and iPSC (Tic) derived definitive endoderms (day 0, 5, 6, and 12). The cells were transduced with Ad-LacZ or Ad-HEX at day 6 as described in **Figure 1a**. The data at day 6 was obtained before the transduction with Ad-HEX. The graphs represent the relative gene expression levels when the level in the fetal liver was taken as 100. (**e–p**) Immunocytochemistry of AFP, ALB, and CK7 expression in nontransduced cells (**e,h,k,** and **n**), Ad-LacZ-transduced cells (**f,i,l,** and **o**), and Ad-HEX-transduced cells (**g,j,m,** and **p**) at day 12, all of which were induced from the human ESC (khES1)- and iPSC (Tic) derived definitive endoderms. Nuclei were stained with DAPI. Bar = 50 μm. Ad, adenovirus; AFP, α-fetoprotein; ALB, albumin; CK7, cytokeratin 7; HEX, Ad-HEX-transduced cells; ESC, embryonic stem cells; iPSC, induced pluripotent stem cell; LacZ, Ad-LacZ-transduced cells; None, nontransduced cells.

transduced cells and nontransduced cells. At day 7 (the day after transduction), the expression of AFP was not detectable in Ad-HEX-transduced or nontransduced cells (**Supplementary Figure S5a,d**). At day 8–9, morphological changes to hepatocyte-like cells were observed in Ad-HEX-transduced cells (**Supplementary Figure S5h,i**). We also observed homogeneous AFP-positive cells at day 9 (**Supplementary Figure S5e**). At day 10, CK7-positive cells appeared, indicating that hepatoblasts started to differentiate into hepatocytes and cholangiocytes at day 9–10 (**Supplementary Figure S5f**). At day 12, ALB-positive cells appeared, indicating that hepatocytes were differentiated from Ad-HEX-transduced cells (**Figure 4p**). These results showed that *HEX* induces the hepatoblasts from the

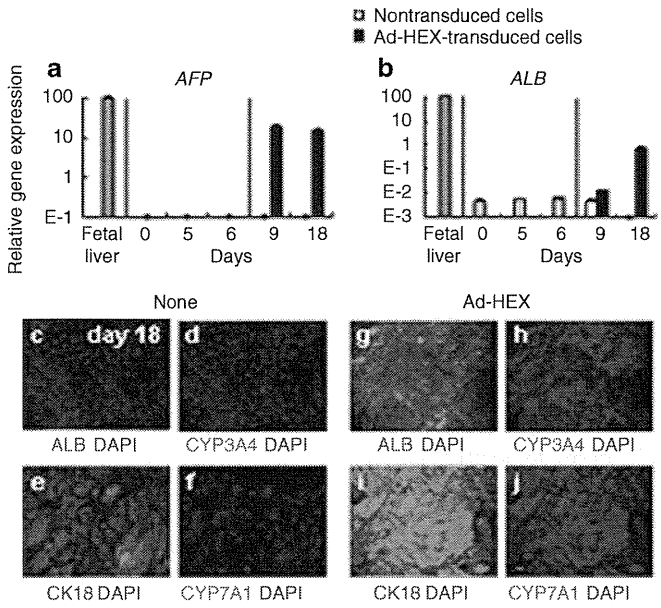

Figure 5 Efficient differentiation of Ad-HEX-transduced hepatoblasts into hepatocytes. (**a**,**b**) Real-time RT-PCR analysis of (**a**) *AFP* and (**b**) *ALB* expression in nontransduced cells and Ad-HEX-transduced cells, both of which were induced from the human iPSC (Tic) derived definitive endoderm (day 0, 5, 6, and 12). The cells were transduced with Ad-HEX at day 6 as described in **Figure 1a**. The data at day 6 were obtained before the transduction with Ad-HEX. The graphs represent the relative gene expression level when the level in the fetal liver was taken as 100. (**c–j**) Immunocytochemistry of ALB, CYP3A4, CYP7A1, and CK18 expression in (**c–f**) nontransduced cells and (**g–j**) Ad-HEX-transduced cells, all of which were induced from the human iPSC (Tic) derived definitive endoderm at day 18. Nuclei were stained with DAPI. Bar = 50 μm. Ad, adenovirus; AFP, α-fetoprotein; ALB, albumin; CK18, cytokeratin 18; ESC, embryonic stem cells; HEX, Ad-HEX-transduced cells; iPSC, induced pluripotent stem cell; None, nontransduced cells; RT-PCR, reverse transcriptase-PCR.

definitive endoderm, and the Ad-HEX-transduced cells could differentiate into both hepatocytes and cholangiocytes.

Directed hepatic differentiation from hepatoblasts

With the protocol described above, heterogeneous populations containing CK7-positive cholangiocytes were observed at day 12 (**Figure 4p**). To promote the differentiation of hepatoblasts to hepatocytes, the human iPSC-derived differentiated cells at day 9 (**Supplementary Figure S5e**) were dislodged with trypsin-EDTA and plated on collagen I-coated dishes as previously reported.[11] After 8–11 days in culture with medium containing FGF4, HGF, OSM, and DEX, the Ad-HEX-transduced cells became more flattened (**Supplementary Figure S5m**), whereas the nontransduced cells became fibroblast-like cells (**Supplementary Figure S5i**). Gene expression analysis showed the upregulation of *ALB* mRNA in Ad-HEX-transduced cells under this culture condition, whereas the expression of *ALB* mRNA was reduced in the nontransduced cells at day 18 (**Figure 5b**). Immunostaining showed that only a small percentage of Ad-HEX-transduced cells expressed ALB at day 12 (**Figure 4p**), whereas most of the Ad-HEX-transduced cells were ALB-positive at day 18 (**Figure 5g**). Most of the Ad-HEX-transduced cells also expressed CYP3A4 at day 18 (**Figure 5h**). More importantly, in the Ad-HEX-transduced cells, CYP7A1 and cytokeratin 18 were detected and these proteins are known

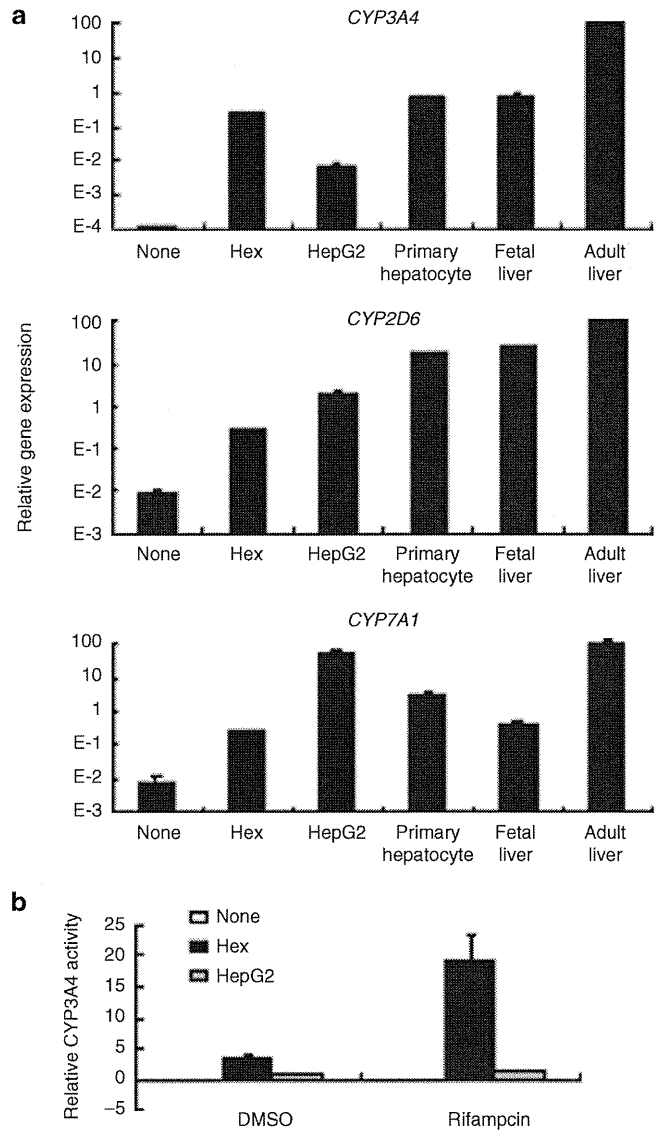

Figure 6 Cytochrome P450 isozymes in human iPSC (Tic) derived hepatocytes. (**a**) Real-time RT-PCR analysis of *CYP3A4*, *CYP7A1*, and *CYP2D6* expression in iPSC (Tic) derived nontransduced cells, Ad-HEX-transduced cells, and fetal and adult liver tissues. (**b**) Induction of CYP3A4 by rifampicin in human iPSC (Tic) derived nontransduced cells, Ad-HEX-transduced cells, the HepG2 cell line and primary human hepatocytes, which were cultured 48 hours after plating the cells. Data are presented as the mean ± SD from triplicate experiments. The graphs represent the relative gene expression level when the level in the adult liver was taken as 100. AFP, α-fetoprotein; ALB, albumin; DMSO, dimethyl sulfoxide; ESC, embryonic stem cells; HEX, Ad-HEX-transduced cells; iPSC, induced pluripotent stem cell; LacZ, Ad-LacZ-transduced cells; None, nontransduced cells.

to be detected in hepatocytes but not in extra-embryonic cells[31,32] (**Figure 5i,j**). Quantitative analysis showed that ~84, 80, 88, and 92% of Ad-HEX-transduced cells expressed ALB, CYP3A4, CYP7A1, and cytokeratin 18, respectively. These results indicate that Ad-HEX-transduced cells could differentiate to hepatic cells. However, the expression level of *ALB* mRNA in Ad-HEX-transduced cells was lower than that in fetal liver tissue and in turn, the expression of *AFP* mRNA was maintained (**Figure 5a**). Therefore, Ad-HEX-transduced cells are committed to the hepatic linage, but are not yet mature hepatocytes.

Ad-HEX-transduced cells exhibit hepatic functions

To test the hepatic function in the Ad-HEX-transduced cells, we investigated the liver metabolism, because P450 cytochrome enzymes play a critical role in this function. We examined the expression level of several members of this multigene family, *i.e.*, *CYP3A4*, *CYP7A1*, mRNA and *CYP2D6* in Ad-HEX-transduced cells by real-time RT-PCR. The real-time RT-PCR analysis showed that the mRNAs for *CYP3A4*, *CYP7A1*, and *CYP2D6* were expressed in Ad-HEX-transduced cells, whereas none of these mRNAs were expressed in the nontransduced cells (**Figure 6a**). The expression levels of *CYP3A4* in Ad-HEX-transduced cells were similar to those observed in primary human hepatocytes, which were cultured 48 hours after plating the cells, or fetal liver tissues but lower than those in adult liver. The *CYP2D6* and *CYP7A1* mRNA expressions in Ad-HEX-transduced cells were lower than those in primary hepatocytes or adult tissues. Next, we investigated the metabolism of the P450 3A4 substrates by measuring the activity of P450 isozymes. The metabolites were detected in Ad-HEX-transduced cells, and their activity was 3.4-fold higher than that in the most commonly used human hepatocyte cell line, HepG2 (**Figure 6b**; DMSO column). This result was consistent with the real-time RT-PCR data (**Figure 6a**). We further tested the induction of CYP3A4 upon chemical stimulation, because CYP3A4 is the most prevalent P450 isozyme in the liver and is involved in the metabolism of a significant proportion of the currently available commercial drugs. Because CYP3A4 can be induced with rifampicin, both Ad-HEX-transduced cells and HepG2 cells were treated with rifampicin, followed by treatment with CYP3A4 substrate. Ad-HEX-transduced cells produced 5.4-fold higher levels of metabolites in response to rifampicin treatment (**Figure 6b**; rifampicin column). This result indicates that P450 isozymes are active in Ad-HEX-transduced cells.

DISCUSSION

The object of this study was to develop an efficient method for generating hepatoblasts and hepatocytes from human ESCs and iPSCs for application to drug toxicity screening tests as well as therapeutics such as regenerative medicine. We found that transient HEX transduction in the definitive endoderm together with a culture under chemically defined conditions was useful for this purpose.

It has been reported that a high concentration of Activin A induces differentiation of human ESCs into the definitive endoderm.[8,33,34] On the other hand, undifferentiated human ESCs are maintained by a low concentration of Activin A.[35] Several studies have shown that bFGF promotes the differentiation of ESCs into the definitive endoderm and inhibits the differentiation of ESCs into the extra-embryonic endoderm.[35–38] bFGF has been reported to inhibit the BMP signaling, which can promote the extra-embryonic lineage differentiation.[39] The extra-embryonic endoderm expresses most of the hepatocyte markers, such as AFP.[40] Contamination of the extra-embryonic endoderm makes it difficult to estimate the hepatic differentiation from human ESCs and iPSCs.[11,14,40] In this study, we showed that both Activin A and bFGF induce definitive endoderm populations, while they repress the extra-embryonic endoderm differentiation (**Figure 2g,h**). Interestingly, after the differentiated cells that were cultured on laminin-coated plates with Activin A and bFGF were passaged at day 5, FOXA2-positive cells (definitive endoderm) were enriched in the resultant cells at day 6 (**Figure 2a–f**). This may have been because FOXA2-positive cells efficiently adhered to the laminin-coated plate and/or because trypsinized, single undifferentiated ESCs/iPSCs cannot survive. The passaging of differentiated cells might be attributed to the reduction in the number of not only the extra-embryonic endoderm cells but also the undifferentiated cells. However, the efficiency of the definitive endoderm differentiation in this study was not as efficient as that reported by other groups.[8,33,34] Other cell lineages, such as the mesoderm and extra-embryonic endoderm, might remain at day 6 (**Figure 2g,h** and **Supplementary Figure S1**). Further improvement of the culture conditions will thus be needed in order to enhance the definitive endoderm differentiation.

Hepatoblasts and hepatocytes were differentiated from the human ESC- and iPSC-derived definitive endoderms by transient overexpression of the homeobox gene *HEX*. A fiber-modified Ad vector containing K7 peptides mediated much higher gene expression than conventional Ad vectors in the human ESC- and iPSC-derived definitive endoderms (**Supplementary Figure S6**). This new hepatic differentiation protocol shows that *HEX* induces AFP-positive hepatoblasts at day 9 and ALB-positive hepatocytes at day 12 from human ESCs and iPSCs, whereas the previous protocols require a few weeks or months to induce AFP- and ALB-positive hepatocytes from PSCs.[9–11] Previous studies suggested that *HEX* could regulate liver-enriched transcription factors such as hepatocyte nuclear factor 4A and hepatocyte nuclear factor 6.[19,23] Overexpression of the *HEX* gene under the conditions employed in the present study could activate several transcription factors that are required for hepatic differentiation (**Supplementary Figure S4a,b**). However, the Ad-HEX-transduced cells showed a low level of expression of *ALB* and some CYP450 species, as well as a high level of *AFP* expression, indicating that the cells were still immature. To promote further hepatic differentiation or maturation, it may be effective to culture the hepatic cells in a 3D environment or on feeder cells such as cardiomyocyte- or endothelium-derived cells.[41,42] In addition, the function of our hepatic cells was still limited. Further analysis of the other functions of our hepatic cells, such as glycogen storage, uptake of indocyanine green and organic anion low-density lipoprotein, and transplantation of Ad-HEX-transduced cells into the liver of immunodeficient mice, is clearly needed for the appreciation to drug screening and therapeutic treatment modalities.

During the preparation of this article, Kubo *et al.* have reported that *HEX* could promote hepatoblast differentiation from mouse ESCs.[43] Their report is consistent with our data, suggesting that *HEX* plays a pivotal regulatory role in not only mouse but also human hepatic differentiation. They also showed that the overexpression of *HEX* at the definitive endoderm stage is critical for hepatic specification of the mouse ESCs. We also confirmed that forced expression of *HEX* in the undifferentiated human ESCs and iPSCs did not elevate the expression of *ALB* and *CK7* (**Supplementary Figure S7**), indicating that *HEX* enhances the hepatic differentiation not from the undifferentiated cells but from the definitive endoderm. However, Kubo *et al.* used recombinant mouse ESCs (tet-HEX ESCs), in which the tetracycline-regulated *HEX* expression cassette

is integrated into the host cell genome to induce *HEX* in a stage-specific manner. Their system would not be appropriate for clinical use because the transgene is randomly integrated into the host cell genome and this leads to a risk of mutagenesis.[44] On the other hand, we generated human hepatoblasts by Ad vector-mediated transient *HEX* transduction, method which avoids the integration of exogenous DNA into the host chromosome.

Touboul *et al.* reported that human ESCs and iPSCs can differentiate into functional hepatocytes under chemically defined conditions.[34] In the present study, hepatoblasts were generated in a chemically defined serum-free medium, which minimized exposure to animal cells and proteins, and on a defined extracellular matrix, such as laminin or collagen, which do not contain undefined growth factors. To generate hepatocytes, hepatocyte culture medium, which is serum-free but not defined, was used in the stage III. When defined hESF-medium was used in the stage III, the expression levels of *ALB* and *CYP3A4* mRNA were half the levels seen in the cells cultured with hepatocyte culture medium in the preliminary experiment (data not shown). Human ESCs and iPSCs were also grown for maintaining the undifferentiated state on a feeder layer, which contains xenoantigen such as bovine apolipoprotein B-100. Bovine apolipoprotein B-100 is known to be a dominant xenoantigen for cell-based therapies.[45] Human ESC- and iPSC-derived hepatocytes should be generated and cultured under chemically defined conditions not only to avoid potential contamination with pathogens for the safer therapeutic application, but also to obtain reproducible results using the differentiation protocols.[34,46] Development of differentiation protocols using other genes of transcription factors as well as *HEX* genes based on a chemically defined medium is under way. Overall, our strategy should provide a novel protocol for hepatic differentiation from human ESCs and iPSCs, which could be useful for regenerative medicine and drug screening.

MATERIALS AND METHODS

Ad vectors. Ad vectors were constructed by an improved *in vitro* ligation method.[47,48] The human *HEX* complementary DNA derived from pDNR-LIB-*HEX* (Invitrogen, Carlsbad, CA) was inserted into pHMEF5,[29] which contains the human elongation factor-1α promoter, resulting in pHMEF-HEX. The pHMEF-HEX was digested with I-CeuI/PI-SceI and ligated into I-CeuI/PI-SceI-digested pAdHM41-K7,[30] resulting in pAd-HEX. Ad-HEX and Ad-LacZ, both of which contain the elongation factor-1α promoter and a stretch of lysine residues (K7) peptides in the C-terminal region of the fiber knob, were generated and purified as described previously.[26,29] The vector particle titer was determined by using a spectrophotometric method.[49]

Human ESCs and iPSCs culture. A human ESC line, khES1, was obtained from Kyoto University (Kyoto, Japan).[50] khES1 was used following the Guidelines for Derivation and Utilization of Human Embryonic Stem Cells of the Ministry of Education, Culture, Sports, Science and Technology of Japan after approval by the review board at Kyoto University. Human ESCs were maintained on a feeder layer of mitomycin-inactivated mouse embryonic fibroblasts (ICR; ReproCELL Incorporated, Tokyo, Japan) with Dulbecco's modified Eagle's medium/F-12 (Sigma, St Louis, MO) supplemented with 0.1 mmol/l 2-mercaptoethanol, 0.1 mmol/l nonessential amino acids, 2 mmol/l L-glutamine, 20% GIBCO knockout serum replacement (Invitrogen), and 5 ng/ml bFGF (Sigma) in a humidified atmosphere of 3% CO_2 and 97% air at 37 °C. Human ESCs were dissociated with 0.1 mg/ml dispase (Roche Diagnostics, Burgess Hill, UK) into small clumps, and subcultured every 5 or 6 days.

Two human iPS clones derived from the embryonic human lung fibroblast cell line MCR5 were provided from JCRB Cell Bank (Tic, JCRB Number: JCRB1331; and Dotcom, JCRB Number: JCRB1327).[3,4] In the present study, we mainly used the Tic cell line, but similar results were obtained using the Dotcom cell line, and these are shown in the supplementary figures. Human iPSCs were maintained on a feeder layer of mitomycin-inactivated mouse embryonic fibroblasts (Hygro Resistant Strain C57/BL6; Hygro, Millipore, MA) on a gelatin-coated flask in human iPS medium. Human iPS medium consists of knockout Dulbecco's modified Eagle's medium/F12 (Invitrogen), supplemented with 0.1 mmol/l 2-mercaptoethanol, 0.1 mmol/l nonessential amino acids, 2 mmol/l L-glutamine, 20% knockout serum replacement, and 10 ng/ml bFGF in a humidified atmosphere of 5% CO_2 and 95% air at 37 °C. Human iPSCs were dissociated with 0.1 mg/ml dispase (Roche) into small clumps and subcultured every 7 or 8 days.

In vitro *differentiation.* Before the initiation of cellular differentiation, the medium of human ESCs and iPSCs was exchanged for a defined serum-free medium hESF9 and cultured in a humidified atmosphere of 10% CO_2 and 90% air at 37 °C.[46] hESF9 consists of hESF-GRO medium (Cell Science & Technology Institute, Sendai, Japan) supplemented with five factors (10 μg/ml human recombinant insulin, 5 μg/ml human apotransferrin, 10 μmol/l 2-mercaptoethanol, 10 μmol/l ethanolamine, 10 μmol/l sodium selenite), oleic acid conjugated with fatty acid free bovine ALB, 10 ng/ml bFGF, and 100 ng/ml heparin (all from Sigma). For induction of definitive endoderm, human ESCs and iPSCs were dissociated into single cells with Accutase (Invitrogen) and cultured for 5 days on a mouse laminin-coated tissue 12-well plate (6.0×10^4 cells/cm^2) in hESF-GRO medium (Cell Science & Technology Institute) supplemented with the five factors, 0.5 mg/ml fatty acid free bovine ALB (BSA) (Sigma), 10 ng/ml bFGF, and 50 ng/ml Activin A (R&D Systems, Minneapolis, MN) in a humidified atmosphere of 10% CO_2 and 90% air at 37 °C. The medium was refreshed every day.

For induction of hepatoblasts, the human ESC- and iPSC-derived definitive endoderms (day 5) were dissociated with 0.0125% trypsin-0.01325 mmol/l EDTA, and then the trypsin was inactivated with 0.1% soybean trypsin inhibitor (Sigma). The cells were seeded at 1.2×10^5 cells/cm^2 on a laminin-coated 12-well plate with hESF-DIF (Cell Science & Technology Institute) medium supplemented with the five factors, 0.5 mg/ml BSA, 10 ng/ml bFGF, and 50 ng/ml Activin A in a humidified atmosphere of 10% CO_2 and 90% air at 37 °C. The next day, the cells were transduced with 3,000 vector particle/cell of Ad vectors (Ad-HEX and Ad-LacZ) for 1.5 hours in hESF-DIF medium supplemented with the five factors, BSA, 10 ng/ml FGF4 (R&D Systems) and 10 ng/ml BMP4 (R&D Systems).[10] The medium was refreshed every day.

For induction of hepatocytes, human iPSC-derived hepatoblasts in one well (day 9) were passaged onto two wells with 0.0125% trypsin-0.01325mmol/l EDTA and 0.1% trypsin inhibitor, on type I collagen-coated tissue 12-well plate (15 μg/cm^2) (Nitta Gelatin, Osaka, Japan). The cells were cultured in hepatocyte culture medium supplemented with SingleQuots (Lonza, Walkersville, MD), 10 ng/ml FGF4, 10 ng/ml HGF (R&D Systems), 10 ng/ml Oncostatin M (R&D Systems), and 0.392 ng/ml dexamethasone (Sigma).[11] The medium was refreshed every 2 days.

RNA isolation, RT-PCR, immunostaining, flow cytometry, lacz assay, and assay for cytochrome P4503A4 activity. For details of these procedures, See **Supplementary Materials and Methods, Supplementary Tables S1 and S2.**

SUPPLEMENTARY MATERIAL

Figure S1. Characterization of the human ESC (khES1)- and iPSC (Tic)-derived definitive endoderms.

Figure S2. Efficient differentiation of another human iPSC line (Dotcom) into hepatoblasts by overexpression of the *HEX* gene.

Figure S3. Overexpression of *HEX* in the human ESC (khES1)- and iPSC (Tic)-derived definitive endoderms.